

# Macromolecules

Volume 28, Number 18

August 28, 1995

© Copyright 1995 by the American Chemical Society

## Polymerization of $\epsilon$ -Caprolactone Initiated by Aluminum Isopropoxide Trimer and/or Tetramer

Andrzej Duda\* and Stanislaw Penczek\*

Department of Polymer Chemistry, Center of Molecular and Macromolecular Studies,  
Polish Academy of Sciences, Sienkiewicza 112, 90-363 Lodz, Poland

Received February 13, 1995; Revised Manuscript Received May 30, 1995\*

**ABSTRACT:** Polymerization of  $\epsilon$ -caprolactone ( $\epsilon$ CL) initiated with aluminum isopropoxide ( $\text{Al}(\text{O}^i\text{Pr})_3$ ) trimer ( $A_3$ ), tetramer ( $A_4$ ), or both has shown that these two aggregates react with  $\epsilon$ CL with different rates ( $k_{i3}/k_{i4} \approx 10^3$ , where  $k_{i3}$  and  $k_{i4}$  denote the rate constants of initiation with  $A_3$  and  $A_4$ , respectively). Moreover, the  $^1\text{H}$  NMR measurements revealed relatively low rates of  $A_3 \rightleftharpoons A_4$  interconversion in their diluted solutions: the initial rates of  $A_4 \rightarrow A_3$  and  $A_3 \rightarrow A_4$  conversions were found to be equal to 0.015 and 0.04 mol % $\cdot$ h $^{-1}$  at 25 °C, and to 1.3 and 0.1 mol % $\cdot$ h $^{-1}$  at 70 °C, respectively ( $[\text{Al}(\text{O}^i\text{Pr})_3]_0 = 0.1 \text{ mol}\cdot\text{L}^{-1}$ , benzene solutions). Therefore, when an  $A_3/A_4$  mixture is used in  $\epsilon$ CL polymerization,  $A_3$  is consumed completely whereas  $A_4$  remains unreacted, at least within the time required for the complete  $\epsilon$ CL polymerization. In the initiator reacted with  $\epsilon$ CL, all three  $\text{O}^i\text{Pr}$  groups from  $\text{Al}(\text{O}^i\text{Pr})_3$  are transferred into the poly( $\epsilon$ CL) macromolecules as the end groups. Molecular weights ( $\bar{M}_n$ ) calculated with an assumption that in the involved active centers three poly( $\epsilon$ CL) chains grow from one Al atom agree well with  $\bar{M}_n$  determined by gel permeation chromatography and the end group analysis ( $^1\text{H}$  NMR) for the polymers deactivated with  $\text{HCl}_{\text{aq}}$ .  $\bar{M}_w$  of the living poly( $\epsilon$ CL), determined by multiangle laser light scattering revealed, after comparison with  $\bar{M}_n$  and  $\bar{M}_w/\bar{M}_n$  data for the deactivated poly( $\epsilon$ CL), that the growing species assumes the nonaggregated (monomeric) three-armed structure:  $\text{Al}\{[-\text{O}(\text{CH}_2)_5\text{C}(\text{O})]_n-\text{OCH}(\text{CH}_3)_2\}_3$  ( $P_n^*$ ).  $^{27}\text{Al}$  NMR spectra of the living poly( $\epsilon$ CL) suggest that, at least in a certain fraction of  $P_n^*$ , the additional coordination of the Al atoms by the acyl oxygen atoms of the polymer repeating units takes place. Thus, the tetra-, penta-, and hexacoordinated Al atoms coexist during polymerization. Studies of the polymerization kinetics allowed the  $\epsilon$ CL propagation rate constants on the  $>\text{Al}-\text{OCH}_2-\dots$  active species  $k_p = 0.62 \text{ mol}^{-1}\cdot\text{L}\cdot\text{s}^{-1}$  to be determined (THF, 25 °C). This rate constant refers to the total concentration of the active species of various coordination numbers.

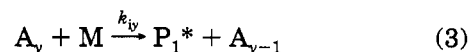
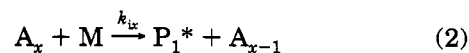
### Introduction

Aluminum alkoxides ( $\text{R}_{3-n}\text{Al}(\text{OR})_n$ ) have been used as initiators in polymerization of cyclic esters for over thirty years.<sup>1–11</sup> Both trialkoxides ( $\text{Al}(\text{OR})_3$ )<sup>1,3,4,8,10,11</sup> and dialkyl alkoxides ( $\text{R}_2\text{AlOR}'$ )<sup>2,5–7,9</sup> have been applied.

The aluminum alkoxides are known to exist at least as dimers, trimers, and tetramers.<sup>12–14</sup> Although these various aggregates may behave differently in initiation, due to their various reactivities, this problem has only been undertaken in our short presentation<sup>15</sup> and the following note,<sup>16</sup> where we have suggested that aluminum triisopropoxide ( $\text{Al}(\text{O}^i\text{Pr})_3$ ) trimer ( $A_3$ ) and tetramer ( $A_4$ ) react with  $\epsilon$ -caprolactone ( $\epsilon$ CL) at different rates. In these notes, the evidence of this difference in initiation rates with  $A_3$  and  $A_4$  has mostly been based on analysis of the  $^1\text{H}$  NMR spectra; they differ sufficiently for  $A_3$  and  $A_4$ , allowing the reaction of these

two aggregates with  $\epsilon$ CL to be followed separately.<sup>16</sup>

The difference of reactivities between species of different aggregation degrees is a general problem, particularly in initiation with easily aggregating metal alkoxides.<sup>12–14</sup> It can be illustrated with the following kinetic scheme:



in which  $k_{ix} \neq k_{iy}$ , and  $k_{ix}[\text{M}]$  and  $k_{iy}[\text{M}] > k_{xy}[\text{A}_x]^{y-1}$  and  $k_{yx}[\text{A}_y]^{x-1}$  (where  $A_x$  and  $A_y$  refer to two different aggregates with the aggregation degrees  $x$  and  $y$ , respectively;  $P_1^*$  is the first active species, formed

\* Abstract published in *Advance ACS Abstracts*, August 1, 1995.

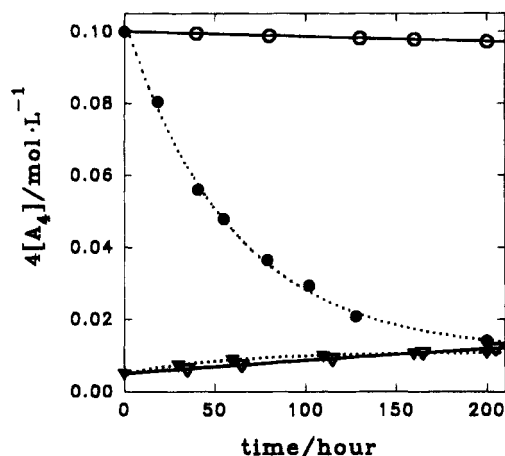


**Figure 1.** Kinetics of  $A_3 \rightarrow A_4$  and  $A_4 \rightarrow A_3$  conversions. Reaction conditions:  $[Al(OiPr)_3]_0 = 3[A_3] + 4[A_4] = 0.1 \text{ mol}\cdot\text{L}^{-1}$ , and benzene- $d_6$  as a solvent, ( $\nabla$ , —)  $A_3 \rightarrow A_4$ , 25 °C; ( $\triangledown$ , —)  $A_3 \rightarrow A_4$ , 70 °C; ( $\circ$ , —)  $A_4 \rightarrow A_3$ , 25 °C; ( $\bullet$ , ···):  $A_4 \rightarrow A_3$ , 70 °C.  $[A_4]$  calculated from the relative intensity of the  $^1\text{H}$  NMR signals due to  $A_4$  in a spectrum of the  $A_3/A_4$  mixture (for details see ref 16).

during initiation, and  $M$  is the monomer;  $k_{xy}$ ,  $k_{yx}$ ,  $k_{ix}$ , and  $k_{iy}$  denote the respective rate constants). The general mathematic treatment of the scheme described by eqs 1–3 will be given elsewhere.<sup>17</sup>

In the present work, we give further evidence for the difference of reactivities of  $A_3$  and  $A_4$ , based on the molecular weight measurements,  $^{27}\text{Al}$  NMR, and polymerization kinetics. Besides, the direct studies of the growing species (NMR and light scattering) allowed us to propose the structure of the growing species, in which three chains grow from one aluminum atom, preventing the active species from aggregation at the stage of propagation.

This result agrees well with a previous observation, mostly by the Jérôme and Teyssié group, indicating that polymerization of  $\epsilon\text{CL}$  with  $Al(OiPr)_3$  is first order in initiator.<sup>3,4</sup> However, earlier reports on the number of growing macromolecules per one Al atom are contradictory. Values from 0.9 to 1.4 for the polymerization carried out in toluene solution at  $[\epsilon\text{CL}]_0 = 1.0 \text{ mol}\cdot\text{L}^{-1}$  in the temperature range from 0 to 100 °C were reported,<sup>18</sup> although Kricheldorf et al.<sup>8</sup> did observe a value of 3 in bulk at 100 °C. Results described in the present work allow an explanation these differences.

## Experimental Section

**Substrates and Solvents.**  $\epsilon$ -Caprolactone (from Aldrich, Steinheim, Germany), THF (from POCh, Gliwice, Poland), and benzene- $d_6$  (from Świerk, Warsaw, Poland) were purified and used according to the described procedures.<sup>6,7</sup> Aluminum isopropoxide trimer ( $A_3$ ) and tetramer ( $A_4$ ) and their mixtures were prepared from the commercially available initiator (from POCh) as was recently described in our work.<sup>16</sup>

**Polymerizations.** Reaction mixtures were prepared using the standard high-vacuum technique. Kinetics of polymerization was studied in vacuum dilatometers.<sup>19</sup>

**NMR Measurements.**  $^1\text{H}$  NMR spectra were recorded in dry benzene- $d_6$  on a Bruker AC200 or Bruker MSL300 apparatus operating at 200 or 300 MHz, respectively. The nondeuterated benzene was used as an internal standard ( $\delta = 7.16 \text{ ppm}$ ).

$^{27}\text{Al}$  NMR spectra were recorded on Bruker MSL 300 apparatus, equipped with a multinuclear probe head and operating at 75 MHz. The  $0.1 \text{ mol}\cdot\text{L}^{-1}$  benzene- $d_6$  solution of aluminum acetylacetonate was used as an external standard ( $\delta = 0 \text{ ppm}$ ). The reaction mixtures were prepared and transferred into the NMR tubes under high-vacuum condi-

tions. The NMR tubes were eventually sealed off after freezing their contents with liquid nitrogen.

**Gel Permeation Chromatography (GPC).** GPC measurements were performed using an LKB 2150 HPLC pump and HPLC Waters ultrastayragel ( $10^3$ ,  $5 \times 10^2$ , and  $10^2$ ) columns ( $\bar{M}_n$  up to  $\sim 2 \times 10^4$ ) or Toyo Soda (G4000HXL and G2000HXL) columns ( $\bar{M}_n$  above  $\sim 2 \times 10^4$ ). Wyatt Optilab 903 interferometric refractometer and/or multiangle laser light scattering (MALLS) Dawn F laser photometer (both Wyatt Technology Corp.) were applied as detectors. THF was used as eluent.

**Molecular Weight Measurements.** The number-average molecular weights ( $\bar{M}_n$ ) were measured on a Knauer membrane osmometer in dry toluene. The weight-average molecular weights ( $\bar{M}_w$ ) were determined with a MALLS Dawn F laser photometer (Wyatt Technology Corp.) in THF solvent.

**Preparation of Samples for GPC and  $\bar{M}_w$  Measurements.** GPC and  $\bar{M}_w$  measurements were performed for both living (i.e., without the purposely introduced agent deactivating the growing ends) and deactivated chains ( $\text{HCl}_{aq}$  was applied). The latter were additionally washed three times with diluted HCl and then with distilled water, until a pH of  $\sim 7$  was reached. During this procedure, aluminum alkoxide head groups hydrolyzed, and as will be shown further, three chains were freed from every aluminum atom. The resulting low molecular weight aluminum compounds ( $Al(OH)_3(\text{Cl})_3$ ) were then separated from the polymer. Finally, poly( $\epsilon\text{CL}$ ) was precipitated into cold methyl alcohol and dried under reduced pressure at room temperature to constant weight. For the lower molecular weight samples, after separation of the organic (benzene) and aqueous layers, the benzene solution of the polymer was lyophilized under reduced pressure.

## Results and Discussion

**$^1\text{H}$  NMR Studies. (a) Spectra of the Initiator.**  $^1\text{H}$  NMR spectra of  $A_3$ ,  $A_4$ , and their mixtures have already been described and analyzed in our previous communication.<sup>16</sup>

In the present work, we give some preliminary data on the rates of  $A_3$  and  $A_4$  interconversions, measured by  $^1\text{H}$  NMR. These measurements were performed for  $[Al(OiPr)_3] \leq 0.1 \text{ mol}\cdot\text{L}^{-1}$  at room temperature, i.e., under typical conditions of  $\epsilon\text{CL}$  polymerization. According to the results shown in Figure 1,  $A_3 \rightleftharpoons A_4$  interconversion is a very slow process observed over hours. The initial rates of the  $A_3 \rightarrow A_4$  and  $A_4 \rightarrow A_3$  conversions, at  $[Al(OiPr)_3]_0 = 0.1 \text{ mol}\cdot\text{L}^{-1}$ , were calculated and are collected in Table 1. It follows that the interconversions are not practically seen for at least several hours even at 70 °C, and thus, concentrations of both  $A_3$  and  $A_4$  remain practically constant.

This allowed us to perform the  $^{27}\text{Al}$  NMR experiments (cf. below) at these conditions. Indeed, when starting from  $4[A_4]_0 = 0.1 \text{ mol}\cdot\text{L}^{-1}$ , the equilibrium concentrations are reached in more than 250 h at 70 °C. The formal constant of the  $4A_3 \rightleftharpoons 3A_4$  equilibrium ( $K_{34} = [A_4]^3/[A_3]^4$ ) at 70 °C equals  $0.027 \text{ mol}^{-1}\cdot\text{L}$  and is not far from the value of  $0.017 \text{ mol}^{-1}\cdot\text{L}$  we calculated from the equilibrium concentrations measured by Shiner et al.<sup>20</sup> It differs, however, from  $K_{34} \approx 40 \text{ mol}^{-1}\cdot\text{L}$ , calculated from the data reported recently<sup>21</sup> on the basis of the  $^{27}\text{Al}$  NMR measurements in toluene as solvent. We are aware that the rates of interconversion and the “equilibrium constants” may depend on the solvent used and that more work is needed to understand the chemistry of  $A_3 \rightleftharpoons A_4$  interconversions. For instance, according to Shiner et al.,<sup>20</sup> in the presence of 2-propanol the rate of interconversion increases almost 25 times ( $[Al(OiPr)_3]_0 = 0.74 \text{ mol}\cdot\text{L}^{-1}$ ,  $[i\text{PrOH}]_0 =$

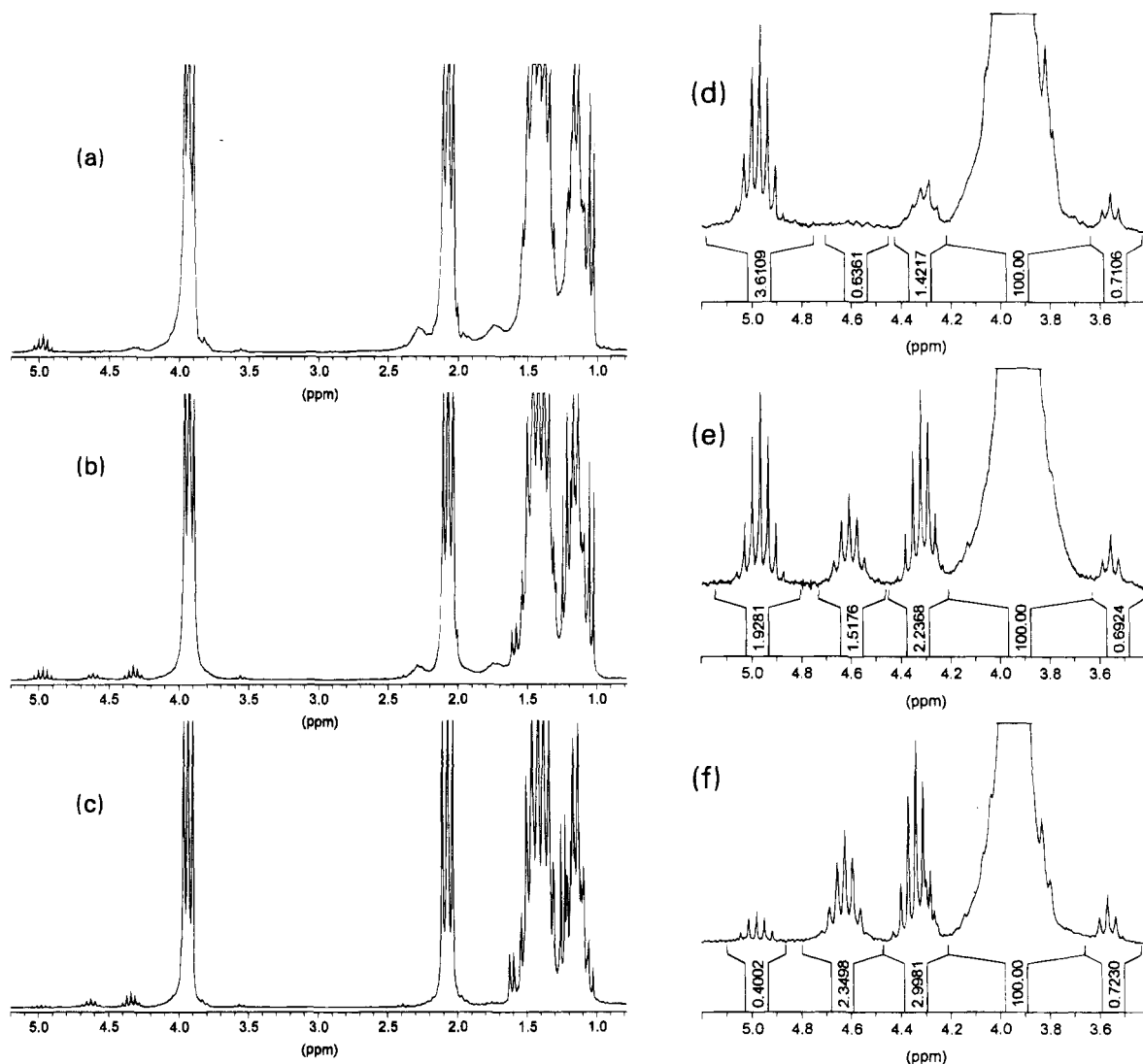


**Figure 2.**  $^1\text{H}$  NMR (200 MHz) spectra of the living poly( $\epsilon\text{CL}$ ). Conditions of polymerization:  $[\epsilon\text{CL}]_0 = 2 \text{ mol}\cdot\text{L}^{-1}$ ,  $[\text{Al}(\text{O}^i\text{Pr})_3]_0 = 3[\text{A}_3]_0 + 4[\text{A}_4]_0 = 0.07 \text{ mol}\cdot\text{L}^{-1}$ , benzene- $d_6$  as a solvent, and  $25^\circ\text{C}$ . (a, d)  $3[\text{A}_3]_0 = 0.065 \text{ mol}\cdot\text{L}^{-1}$ , recorded 20 min after "complete"  $\epsilon\text{CL}$  consumption ( $\leq 5 \text{ min}$ ); (b, e)  $3[\text{A}_3]_0 = 0.0385 \text{ mol}\cdot\text{L}^{-1}$ , recorded 20 min after "complete"  $\epsilon\text{CL}$  consumption ( $\leq 5 \text{ min}$ ); (c, f)  $[\text{A}_3] = "0" \text{ mol}\cdot\text{L}^{-1}$ , recorded 20 min after "complete"  $\epsilon\text{CL}$  consumption ( $\sim 6 \text{ h}$ ).

**Table 1.** Initial Rates of  $\text{A}_3 \rightarrow \text{A}_4$  ( $r_{34}$ ) and  $\text{A}_4 \rightarrow \text{A}_3$  ( $r_{43}$ ) Conversions, Equilibrium Concentrations of  $\text{A}_4$  ( $[\text{A}_4]_{\text{eq}}$ ), and the constants of the  $4\text{A}_3 \rightarrow 3\text{A}_4$  Equilibrium ( $K_{34}$ )<sup>a</sup>

temp ( $^\circ\text{C}$ )	rate ( $\text{mol}\cdot\text{L}^{-1}\cdot\text{h}^{-1}$ )		$4[\text{A}_4]_{\text{eq}} (\text{mol}\cdot\text{L}^{-1})$	$K_{34}^b (\text{mol}^{-1}\cdot\text{L})$
	$r_{34}$	$r_{43}$		
25	0.040	0.015	$\approx 0.035$	3
70	0.100	1.330	0.011	0.027

<sup>a</sup> Measurements by  $^1\text{H}$  NMR. Conditions:  $[\text{Al}(\text{O}^i\text{Pr})_3]_0 = 0.1 \text{ mol}\cdot\text{L}^{-1}$ ,  $\text{C}_6\text{D}_6$ . <sup>b</sup>  $K_{34} = [\text{A}_4]_{\text{eq}}^3/[\text{A}_3]_{\text{eq}}^4 = [\text{A}_4]_{\text{eq}}^3/\{4([\text{A}_4]_0 - [\text{A}_4]_{\text{eq}})/3\}^4$ ;  $[\text{A}_4]$  calculated from the relative intensity of the  $^1\text{H}$  NMR signals due to  $\text{A}_4$  in a spectrum of the  $\text{A}_3/\text{A}_4$  mixture (for details see ref 16).

$1.27 \text{ mol}\cdot\text{L}^{-1}$ , benzene,  $25^\circ\text{C}$ ). Data published by Ropson et al. indicate the same trend.<sup>21</sup> We also observed a similar increase of this rate in the presence of glycols.<sup>22</sup>

However, presented here are the preliminary results of the rates of interconversion, in order to show later that these rates, if measured correctly, are the same when obtained from both  $^1\text{H}$  and  $^{27}\text{Al}$  NMR.

**(b)  $^1\text{H}$  NMR Spectra of the Polymerization Mixtures and of the Isolated Polymers.** In Figure 2 are given the  $^1\text{H}$  NMR spectra recorded during the  $\epsilon\text{CL}$  polymerization ( $\text{C}_6\text{D}_6$ ,  $25^\circ\text{C}$ ) and initiated with  $\text{Al}(\text{O}^i\text{Pr})_3$  ( $[\text{Al}(\text{O}^i\text{Pr})_3]_0 = 3[\text{A}_3]_0 + 4[\text{A}_4]_0 = 0.07 \text{ mol}\cdot\text{L}^{-1}$ ) with  $[\text{A}_3]_0/[\text{A}_4]_0$  ratios equal to 25 (a), 1.5 (b), and "0" (c). The  $[\text{A}_3]_0$  was calculated on a basis of the total amount of  $\text{Al}(\text{O}^i\text{Pr})_3$  used and of the molar fraction of  $[\text{A}_3]$  in the  $\text{A}_3/\text{A}_4$  mixture (the latter determined from the relative

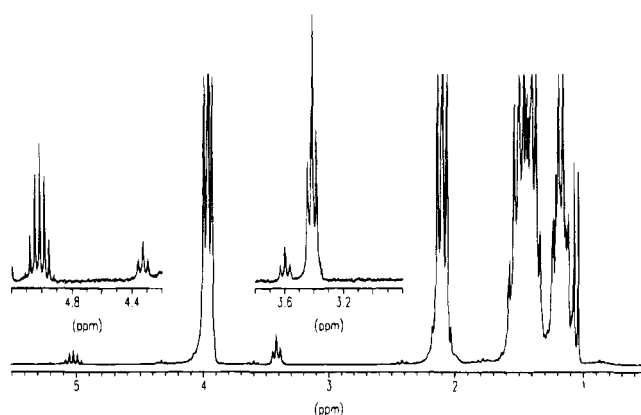
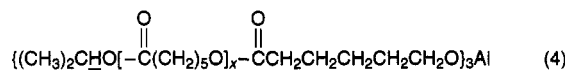
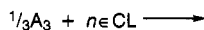


**Figure 3.**  $^1\text{H}$  NMR (200 MHz) spectrum of the isolated poly( $\epsilon\text{CL}$ ) after deactivation of the living polymer with  $\text{HCl}_{\text{aq}}$ . Conditions of polymerizations:  $[\epsilon\text{CL}]_0 = 2 \text{ mol}\cdot\text{L}^{-1}$ ;  $[\text{Al}(\text{O}^i\text{Pr})_3]_0 = 0.07 \text{ mol}\cdot\text{L}^{-1}$ ,  $3[\text{A}_3]_0 = 0.0385 \text{ mol}\cdot\text{L}^{-1}$ , and benzene- $d_6$ ,  $25^\circ\text{C}$ .

$\text{Pr})_3$  ( $[\text{Al}(\text{O}^i\text{Pr})_3]_0 = 3[\text{A}_3]_0 + 4[\text{A}_4]_0 = 0.07 \text{ mol}\cdot\text{L}^{-1}$ ) with  $[\text{A}_3]_0/[\text{A}_4]_0$  ratios equal to 25 (a), 1.5 (b), and "0" (c). The  $[\text{A}_3]_0$  was calculated on a basis of the total amount of  $\text{Al}(\text{O}^i\text{Pr})_3$  used and of the molar fraction of  $[\text{A}_3]$  in the  $\text{A}_3/\text{A}_4$  mixture (the latter determined from the relative

intensity of the  $^1\text{H}$  NMR signals due to  $\text{A}_3$ , just before the polymerization; cf. ref 16). The absorption bands of the  $\text{CH}_2$  main-chain poly( $\epsilon\text{CL}$ ) protons are as follows:  $\delta = 3.93$  (t,  $\epsilon$ ), 2.07 (t,  $\alpha$ ), 1.42 (m,  $\beta + \delta$ ), 1.14 (m,  $\gamma$ ).<sup>3,7,8</sup> The multiplicities and positions with respect to the  $\text{C}(\text{O})\text{O}$  groups are given in parentheses.

$^1\text{H}$  NMR of the methine protons of the initiator and of the resulting polymer chains gives direct insight into the initiator  $\rightarrow$  end group conversion. In agreement with the preliminary data, given in our recent publication,<sup>16</sup> only  $\text{A}_3$  from the  $\text{A}_3/\text{A}_4$  mixture gave the polymer end groups, i.e., initiated polymerization, whereas  $\text{A}_4$  remains unreacted within the time required for complete  $\epsilon\text{CL}$  consumption.

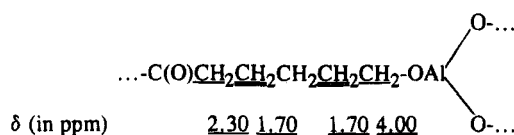


$$\delta = 4.95 \text{ ppm}, n = 3(\bar{x}+1)$$

$$[(\text{CH}_3)_2\text{CHO}]_3\text{Al} \quad \delta \approx 4.30 \text{ ppm (A}_3\text{)}; \delta = 4.30 \text{ and } 4.60 \text{ ppm (A}_4\text{)}$$

NMR traces in Figure 2a–c confirm the expectations: the higher the molar fraction of  $\text{A}_3$  in the  $\text{A}_3/\text{A}_4$  mixture, the more intensive are signals related to the  $(\text{CH}_3)_2\text{CHOC}(\text{O})\cdots$  end groups, namely, the septet at  $\delta = 4.95$  ppm and the doublet at  $\delta = 1.03$  ppm, and the weaker are signals due to the unreacted  $\text{A}_4$  (septets at  $\delta = 4.60$  and  $4.30$  ppm, doublets at  $\delta = 1.60$ ,  $1.30$ , and  $1.23$  ppm). Figure 2d–f give the integrations of the respective signals in the methine protons' absorption range, relative to the intensity of the absorption band due to the poly( $\epsilon\text{CL}$ ) main-chain  $\text{CH}_2\text{OC}(\text{O})$  protons (the latter give relatively strong side bands in the form of triplets at  $\delta = 3.56$  and  $4.32$  ppm).

The broad and small multiplets centered at  $\delta = 2.30$ ,  $1.70$ , and  $\sim 4.0$  ppm (the latter one partially hidden under the main-chain proton signal) may correspond to protons of the methylene groups in the ultimate repeating unit, linked directly to the  $\cdots\text{O}-\text{Al}<$  alkoxide groups. Indeed, their relative intensities decrease with the chain length and thus follow the decrease of the intensities of the  $(\text{CH}_3)_2\text{CHOC}(\text{O})\cdots$  end group signal. Moreover, in the spectra of the poly( $\epsilon\text{CL}$ ) deactivated with aqueous  $\text{HCl}$  (cf. the representative spectrum in Figure 3), these signals disappear and the sharp triplet at  $\delta = 3.45$  ppm appears. This new signal can be ascribed to the  $\cdots\text{C}(\text{O})\text{CH}_2\text{CH}_2\text{CH}_2\text{CH}_2\text{CH}_2\text{OH}$  end groups,<sup>3,7</sup> replacing the  $\cdots\text{C}(\text{O})\text{CH}_2\text{CH}_2\text{CH}_2\text{CH}_2\text{CH}_2\text{OAl}<$  active species. Thus, we tentatively assign the protons and the chemical shifts as shown.



According to the  $^{27}\text{Al}$  NMR spectral analysis, given in the next sections, active species may differ in their coordination numbers of the Al atoms (cf. structures of  $\text{P}_n^*(4)$ ,  $\text{P}_n^*(5)$ , and  $\text{P}_n^*(6)$ ). Superposition of signals related to these various interconverting species gives the observed broad multiplets.

The  $\cdots\text{C}(\text{O})\text{CH}_2\text{CH}_2\text{CH}_2\text{CH}_2\text{CH}_2\text{OAl}(\text{C}_2\text{H}_5)_2$  active species exhibits in the  $^1\text{H}$  NMR exclusively a sharp triplet at  $\delta \approx 3.50$  ppm due to the last methylene

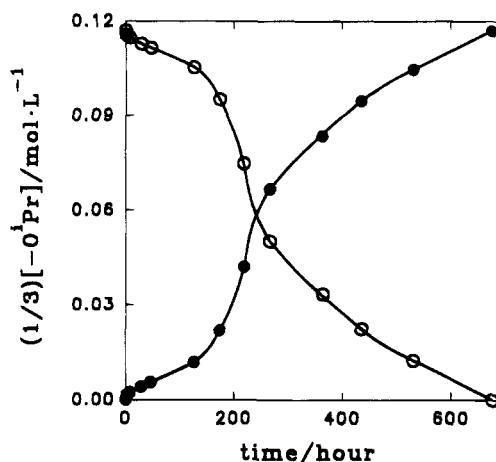


**Figure 4.** Kinetics of slow consumption of  $\text{A}_4$  left after the complete  $\epsilon\text{CL}$  polymerization initiated with  $\text{A}_4$  (polymerization completed within 5 h) and kinetics of the buildup of the polymer end groups. Conditions of polymerization:  $[\epsilon\text{CL}]_0 = 2 \text{ mol}\cdot\text{L}^{-1}$ ,  $4[\text{A}_4]_0 = 0.117 \text{ mol}\cdot\text{L}^{-1}$ , benzene- $d_6$  as a solvent, and  $20^\circ\text{C}$ . (○)  $\text{O}^i\text{Pr}$  groups in  $\text{A}_4$ ; (●)  $\text{O}^i\text{Pr}$  end groups in poly( $\epsilon\text{CL}$ ).

group.<sup>22</sup> The signals of the remaining protons of the active species are overlapped with these of the poly( $\epsilon\text{CL}$ ) main chain.

In the polymerizations initiated with  $\text{A}_4$  alone, only a small fraction of this initiator is reacted (a few percent at the conditions given in Figure 2c) within the time in which  $\epsilon\text{CL}$  is polymerized. However, when the system is kept "living" for a sufficiently long time, all of the  $\text{A}_4$  disappears, reacting with the monomer at equilibrium and/or the polymer repeating units. Also in this instance, all three of the  $\text{O}^i\text{Pr}$  groups linked to one Al atom from initiator ( $\text{A}_4$ ) are converted into the polymer head end groups as with  $\text{A}_3$ , but the required time is exceedingly longer ( $\sim 10^2$  times) than required for  $\epsilon\text{CL}$  to come to the monomer  $\rightleftharpoons$  living polymer equilibrium, when polymerization is initiated with  $\text{A}_3$  alone under comparable conditions. Whether and to what extent a small admixture of  $\text{A}_3$  participated in the  $\epsilon\text{CL}$  polymerization initiated with  $\text{A}_4$  is difficult to estimate at present.

A rough comparison of the rates of initiation with  $\text{A}_3$  and  $\text{A}_4$  gives  $k_{i3}/k_{i4} \approx 10^3$ . A similar ratio of reactivities was determined from the kinetic data given in the next sections.

The slow decrease of concentration of  $\text{A}_4$  ( $[\text{A}_4]$ ) is accompanied by the simultaneous and quantitatively corresponding increase of concentration of the  $\cdots\text{C}(\text{O})\text{OCH}(\text{CH}_3)_2$  end groups, up to the complete consumption of  $\text{A}_4$ . At this point, all of the  $\text{O}^i\text{Pr}$  groups from  $\text{A}_4$  are found in poly( $\epsilon\text{CL}$ ) as the head end groups. The respective kinetic curves are given in Figure 4; the instantaneous concentrations were measured by  $^1\text{H}$  NMR.

**$^{27}\text{Al}$  NMR Studies.** Several attempts have already been made to apply  $^{27}\text{Al}$  NMR spectroscopy to determine the structures of the aluminum alkoxide active centers in polymerization.<sup>21,23–25</sup> However, there are at least two sometimes overlooked phenomena complicating the analysis of the spectra, namely, the quadrupolar character of the  $^{27}\text{Al}$  nuclei and the multinuclear probe head signal.<sup>26</sup>

The former leads to the broad diffuse signals, with the half-height width ( $w_{1/2}$ ) up to  $10^4$  Hz, the neighboring bands overlap, and therefore the accurate integration is difficult or impossible. Indeed, even within a given compound (e.g.,  $\text{A}_4$ ) the ratio of various Al atoms as determined by  $^{27}\text{Al}$  is not equal to the expected one. Thus, for  $\text{A}_4$  this ratio should be equal to 1:3 (hexa- or

tetracoordinate) but it is necessary to carefully find the conditions for measuring the spectra when this ratio becomes equal to 1:3. The hexacoordinate Al atoms give peaks narrow enough (with  $w_{1/2} \approx 10^2$  Hz) at 25 °C, but the tetracoordinate gives diffuse signals. At higher recording temperatures, the resolution is significantly enhanced, but first it has to be ensured that the position of the equilibrium between various coexisting species is not altered. It was shown earlier in this paper that there is a certain temperature "window", at which the rate of interconversion is insignificant and the spectrum is already sharp, and the determined ratio of components is equal to the known (expected) one.

The second factor, namely, the multinuclear probe head signal, becomes particularly important for the diluted samples (e.g.,  $[\text{Al}]_0$  below  $\approx 10^{-1}$  mol·L $^{-1}$ ). This is a typical concentration range of the initiator (or active species) in polymerization, and it requires substantially longer acquisition time. This, in turn, leads to the high intensity of the extraneous probe signal at  $\delta \approx 60$  ppm. In the present work, this difficulty was removed by subtracting the free induction decay signals (FIDs) of the Al-containing sample and of the blank sample, at the otherwise comparable conditions.

In spite of all of these precautions and good results, as it will be shown in the next paragraph, the  $^{27}\text{Al}$  NMR spectra reported in this work were used as a source of information, reconfirming findings, based on the  $^1\text{H}$  NMR. This way, the confirmed  $^1\text{H}$  NMR data were used for the quantitative analysis.

**(a)  $^{27}\text{Al}$  NMR Spectra of the Initiator.** Although  $^{27}\text{Al}$  NMR spectra of  $\text{Al}(\text{O}^i\text{Pr})_3$  were recorded and analyzed several times,<sup>21,27,28</sup> we decided to repeat these measurements in the more diluted solutions (we used  $[\text{Al}(\text{O}^i\text{Pr})_3] \leq 0.10$  mol·L $^{-1}$  vs  $\geq 0.6$  mol·L $^{-1}$  in refs 21, 27, and 28) in order to compare the resulting spectra with these of the polymerizing mixtures.

Figure 5a shows the  $^{27}\text{Al}$  NMR spectrum of  $\text{A}_4$  recorded at 20 °C. It contains two signals: the sharp peak at  $\delta = 1.8$  ppm ( $w_{1/2} = 75$  Hz) and the broad one at  $\delta = 64$  ppm ( $w_{1/2} = 2400$  Hz), resulting from the central, hexacoordinated Al atom ( $\text{Al}_4(6)$ ) and from the three outer, tetracoordinated Al atoms ( $\text{Al}_4(4)$ ), respectively. However, the integration of the  $\text{Al}_4(6)$  and  $\text{Al}_4(4)$  signals give a ratio of intensities well below the expected value of 1:3. In the spectrum of the same  $\text{A}_4$  sample, but recorded at 65 °C (Figure 5b), the signal of  $\text{Al}_4(4)$  is more narrow ( $w_{1/2} = 1360$  Hz) and more intensive. Now, the  $\text{Al}_4(6)$  to  $\text{Al}_4(4)$  intensities ratio is equal to 2.8:1, almost equal to 3:1 as required. We should stress again that, according to the  $^1\text{H}$  NMR spectrum of this sample, the proportion of  $\text{A}_4$  did not change to the extent that we could measure, and no more  $\text{A}_3$  was observed at the end of the NMR measurements than at the beginning. The whole procedure, requiring the sample to be kept at 65 °C, took 20 min.

The  $^{27}\text{Al}$  NMR spectrum of 95%  $\text{A}_3$ , recorded at 20 °C, gives a broad signal ( $w_{1/2} = 2000$  Hz), centered at  $\delta = 35$  ppm (Figure 5c). It was attributed to the central, pentacoordinated Al atom ( $\text{Al}_3(5)$ ).<sup>27</sup> There is also a signal due to some  $\text{Al}_4(4)$  present in the sample at  $\delta = 60$  ppm ( $w_{1/2} = 2500$  Hz). Since the studied sample of  $\text{A}_3$  contains, according to the  $^1\text{H}$  NMR (cf. our previous paper<sup>16</sup>)  $\sim 5$  mol %  $\text{A}_4$  (in  $\text{Al}(\text{O}^i\text{Pr})_3$  ( $\text{A}_1$ ) units) the signal at  $\delta = 64$  ppm refers to the tetracoordinated Al atoms from  $\text{A}_3$  and from  $\text{A}_4$  ( $\text{Al}_3(4)$  and  $\text{Al}_4(4)$ , respectively). The residual signal of  $\text{Al}_4(6)$  is seen at  $\delta = 1.70$  ppm. At 65 °C,  $\text{Al}_3(4)$  and  $\text{Al}_3(5)$  signals become more

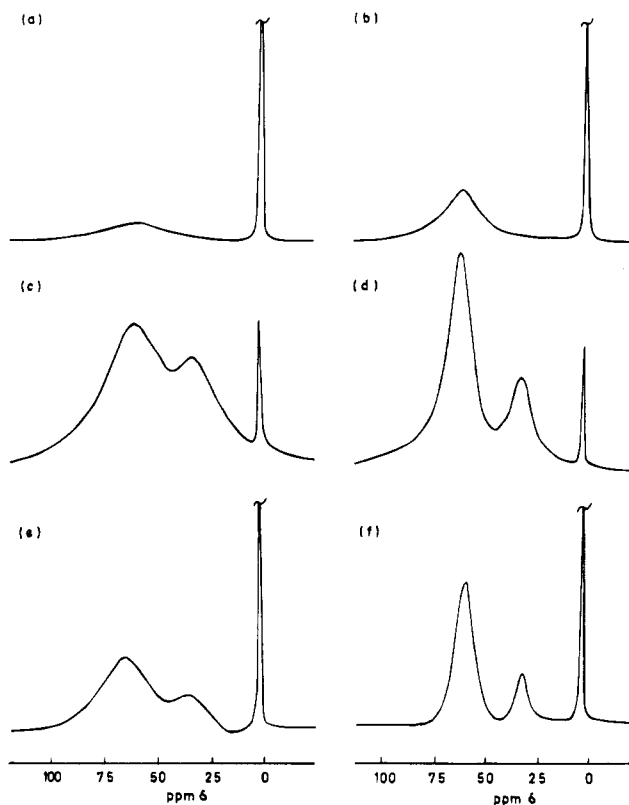


**Figure 5.**  $^{27}\text{Al}$  (75 MHz) NMR spectra of (a) tetrameric  $\text{Al}(\text{O}^i\text{Pr})_3$  ( $\text{A}_4$ ) (20 °C), (b)  $\text{A}_4$  (65 °C), (c) 95% trimeric  $\text{Al}(\text{O}^i\text{Pr})_3$  ( $\text{A}_3$ ) (20 °C), (d) 95%  $\text{A}_3$  (65 °C), (e) equimolar  $\text{A}_3/\text{A}_4$  mixture (20 °C), and (f) (65 °C). Conditions of the measurement:  $[\text{Al}(\text{O}^i\text{Pr})_3]_0 = 3[\text{A}_3]_0 + 4[\text{A}_4]_0 = 0.1$  mol·L $^{-1}$  and benzene- $d_6$  as a solvent.

narrow and better separated (Figure 5d). Thus, for  $\text{Al}_3$  (5)  $w_{1/2}$  decreases to 1000 Hz and the ratio intensities of bands related to  $\text{Al}_3(4)$  and  $\text{Al}_3(5)$  is equal to 2.2:1. This is in a very good agreement with the expected 2:1, taking into account the presence of 5 mol %  $\text{A}_4$ , and giving the calculated ratio equal to 2.16 in place of 2:1 for the pure  $\text{A}_3$ .

Figure 5e shows the  $^{27}\text{Al}$  NMR spectrum of the approximately equimolar  $\text{A}_3/\text{A}_4$  mixture (51/49 molar ratio, with respect to  $\text{A}_1$  units content) recorded at 20 °C. Absorption bands of  $\text{Al}_3(4)$  and  $\text{Al}_4(4)$  are superimposed and partially overlapped with that of  $\text{Al}_3(5)$ . The spectrum of the same  $\text{A}_3/\text{A}_4$  mixture recorded at 65 °C is again much better resolved (Figure 5f). The integration gives  $[\text{Al}_3(5)]/[\text{Al}_4(6)] = 1.29$ , i.e., 49/51 in  $\text{A}_1$  unit terms, close to the ratio determined by  $^1\text{H}$  NMR. Thus,  $([\text{Al}_4(6)] + [\text{Al}_3(5)])/([\text{Al}_4(4)] + [\text{Al}_3(4)]) = 2.49$  is expected, whereas the electronic integration of the  $^{27}\text{Al}$  NMR spectrum yields a slightly lower value, equal to 2.1.

The agreement between the  $^1\text{H}$  and  $^{27}\text{Al}$  NMR spectra of  $\text{A}_3$ ,  $\text{A}_4$ , and their mixtures allows us to use the  $^{27}\text{Al}$  NMR with more confidence in our studies of the polymerizing mixtures.

Let us repeat again, that a single, NMR experiment required  $\sim 20$  min., but within this time, according to our kinetic data (given in the preceding section), no more than a fraction of 1 mol %  $\text{A}_4$  was converted to  $\text{A}_3$  or vice versa. Thus, the concentration changes could be neglected, and an increase in the recording temperature in  $^{27}\text{Al}$  NMR led finally to the correct integration ratios of various Al atoms, i.e.,  $\text{Al}_3(5)$ ,  $\text{Al}_3(4)$ ,  $\text{Al}_4(6)$ , and  $\text{Al}_4(4)$ . Nevertheless, since the changes in the spectra with increasing temperature may look sometimes as

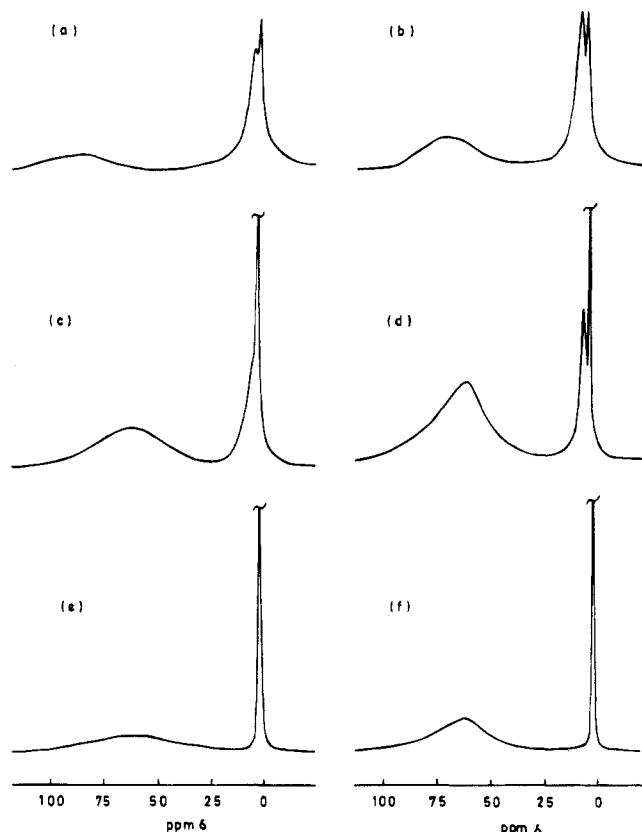


**Figure 6.**  $^{27}\text{Al}$  (75 MHz) NMR spectra of the living poly( $\epsilon\text{CL}$ ). Conditions of polymerization:  $[\epsilon\text{CL}]_0 = 2 \text{ mol}\cdot\text{L}^{-1}$ ,  $[\text{Al}(\text{O}^i\text{Pr})_3]_0 = 3[\text{A}_3]_0 + 4[\text{A}_4]_0 = 0.065 \text{ mol}\cdot\text{L}^{-1}$ , benzene- $d_6$  as a solvent, and 25 °C. (a)  $3[\text{A}_3]_0 = 0.062 \text{ mol}\cdot\text{L}^{-1}$  (20 °C), (b)  $3[\text{A}_3]_0 = 0.062 \text{ mol}\cdot\text{L}^{-1}$  (65 °C), (c) equimolar  $\text{A}_3/\text{A}_4$  mixture (20 °C), (d) equimolar  $\text{A}_3/\text{A}_4$  mixture (65 °C), (e)  $4[\text{A}_4]_0 = 0.065 \text{ mol}\cdot\text{L}^{-1}$  (20 °C) and (f)  $4[\text{A}_4]_0 = 0.065 \text{ mol}\cdot\text{L}^{-1}$  (65 °C).

resulting from a change of composition, it is necessary to ensure by an independent method, e.g., by  $^1\text{H}$  NMR, as it has been done in this paper, that the composition does not change.

**(b)  $^{27}\text{Al}$  NMR Spectra of the Polymerizing Mixtures.** The composition of the polymerizing mixtures was similar to that studied by  $^1\text{H}$  NMR, i.e.,  $[\epsilon\text{CL}]_0 = 2 \text{ mol}\cdot\text{L}^{-1}$ ,  $[\text{Al}(\text{O}^i\text{Pr})_3]_0 = 0.065 \text{ mol}\cdot\text{L}^{-1}$ ,  $\text{C}_6\text{D}_6$  as solvent. Polymerizations were carried out at 25 °C, and the  $^{27}\text{Al}$  NMR spectra were measured at both 20 and 65 °C. All spectra were recorded after the complete consumption of  $\epsilon\text{CL}$ .

In the  $^{27}\text{Al}$  NMR spectra of the poly( $\epsilon\text{CL}$ )-O-Al<, prepared with 95 mol %  $\text{A}_3$  (Figure 6a,b), the  $\text{Al}_3(5)$  signal at  $\delta \approx 30 \text{ ppm}$  is absent. However in the  $\text{Al}(6)$  absorption range, a relatively broad ( $w_{1/2} = 670 \text{ Hz}$  at 20 °C) new signal with  $\delta \approx 5 \text{ ppm}$  has appeared. It can thus be related to the aluminum alkoxide active center. A similar signal was observed earlier for the model  $\gamma$ -butyrolactone (BL)/ $\text{Al}(\text{O}^i\text{Pr})_3$  reaction product and it was attributed to the "mixed tetramer"  $\text{Al}(\text{O}^i\text{Pr})_3\cdot 3\text{BL}$ ,<sup>21</sup> being described as  $\text{Al}(\text{O}^i\text{Pr})_3$  solvated by three molecules of BL allegedly unable to add with a ring opening. At  $\delta = 1.8 \text{ ppm}$ , the  $\text{Al}_4(6)$  peak is present. In the  $\text{Al}(4)$  absorption range, the broad and diffuse signal is seen at 20 °C. It became more narrow and more intensive at 65 °C.

When the  $\text{A}_3/\text{A}_4$  equimolar mixture is used as initiator, the  $\text{Al}(5)$  signal also disappears, as in the system with  $\text{A}_3$  alone, and two overlapped  $\text{Al}(6)$  absorption bands are seen: that at  $\delta = 1.9 \text{ ppm}$  is due to the unreacted  $\text{A}_4$  ( $\text{Al}_4(6)$ ), the second at  $\delta = 5.2 \text{ ppm}$

**Table 2.** Dependence of  $\bar{M}_n$  of Poly( $\epsilon\text{CL}$ ) on  $[\text{A}_3]_0$ <sup>a</sup>

$[\epsilon\text{CL}]_0$ ( $\text{mol}\cdot\text{L}^{-1}$ )	$3[\text{A}_3]_0^b$ ( $10^{-2} \text{ mol}\cdot\text{L}^{-1}$ )	$x[\text{A}_x]_0^c$ ( $10^{-2} \text{ mol}\cdot\text{L}^{-1}$ )	$\bar{M}_n$		
			calcd <sup>d</sup>	GPC <sup>e,f</sup>	NMR <sup>g</sup>
2	0.03	5.18 <sup>g</sup>	1530	1500	1950
2	3.89	2.72	2858	2600	2340
2	"0"	0.55 <sup>h</sup>	13895	14000	
1	6.65	4.21 <sup>g</sup>	964	1080	1140
1	3.85	2.20 <sup>g</sup>	1790	1640	2160
1	"0"	0.40 <sup>h</sup>	9572	10000	

<sup>a</sup> Polymerization Conditions:  $[\text{Al}(\text{O}^i\text{Pr})_3]_0 = 3[\text{A}_3]_0 + 4[\text{A}_4]_0 = 0.07 \text{ mol}\cdot\text{L}^{-1}$ ,  $\text{C}_6\text{D}_6$  as a solvent, 25 °C. <sup>b</sup> Determined from the  $^1\text{H}$  NMR spectra of the  $\text{C}_6\text{D}_6$  initiator solutions. <sup>c</sup>  $[\text{A}_x]_0$  concentrations of the consumed initiator ( $x = 3$  or 4) determined from the final  $^1\text{H}$  NMR spectra, where the  $\text{O}^i\text{Pr}$  groups were observed only in the chain ends and in  $\text{A}_4$ . <sup>d</sup>  $\bar{M}_n(\text{calcd}) = ([\epsilon\text{CL}]_0/3x[\text{A}_x]_0) \times 114.14 + 60.10$  (where 114.14 and 60.10 are the molecular weights of  $\epsilon\text{CL}$  and  $^i\text{PrOH}$ , respectively). <sup>e</sup> Calibrated on the poly( $\epsilon\text{CL}$ ) standards (cf. ref 7). <sup>f</sup> Measured for poly( $\epsilon\text{CL}$ ) deactivated with  $\text{HCl}_{\text{aq}}$  ( $\dots - \text{CH}_2\text{O}(\text{Al}) \rightarrow 3\dots - \text{CH}_2\text{OH}$ ). <sup>g</sup> Polymerization time (up to "complete"  $\epsilon\text{CL}$  consumption)  $\leq 5 \text{ min}$ . <sup>h</sup> Polymerization time (up to "complete"  $\epsilon\text{CL}$  consumption) 6 h.

(chemical shift read at 65 °C), can again be ascribed to the active species as above (Figure 6c,d).

Spectra of the poly( $\epsilon\text{CL}$ )-O-Al< prepared with  $\text{A}_4$  (Figure 6e,f) show, at the moment of monomer consumption, practically only the signal of the unreacted initiator. The weak signal of the active species is probably hidden under the much more intensive bands of  $\text{A}_4$ .

Thus, results of the analysis of the  $^{27}\text{Al}$  NMR spectra of  $\text{Al}(\text{O}^i\text{Pr})_3$  and of  $\epsilon\text{CL}/\text{Al}(\text{O}^i\text{Pr})_3$  polymerizing mixtures reconfirm the main conclusions drawn from the analysis of the  $^1\text{H}$  NMR spectra, namely, that reactivity of  $\text{A}_3$  toward  $\epsilon\text{CL}$  considerably exceeds that of  $\text{A}_4$ .

Another important observation indicates that at least a fraction of the growing species contains the hexacoordinated Al atoms. This finding is discussed later in the paper.

**Dependence of the Poly( $\epsilon\text{CL}$ ) Molecular Weights on the  $[\text{A}_3]_0$ .** As we have already stressed, it was indicated in publications of other authors that from 0.9 to 3.0  $\text{O}^i\text{Pr}$  groups per one Al atom are transferred from  $\text{Al}(\text{O}^i\text{Pr})_3$  to the polymer end groups. This result was puzzling.<sup>8,18</sup>

We have shown already,<sup>15,16</sup> and we provide further confirmation in this paper, that all three groups may be used from  $\text{Al}(\text{O}^i\text{Pr})_3$  derived from both  $\text{A}_3$  and  $\text{A}_4$ . However,  $\text{A}_4$  reacts so much slower than  $\text{A}_3$  that if the mixture of  $\text{A}_3$  and  $\text{A}_4$  is used, then there is not enough time allowed for  $\text{A}_4$  to participate in initiation. Therefore, on average usually less than three  $\text{O}^i\text{Pr}$  groups per one Al atom react if the  $\text{A}_3/\text{A}_4$  mixture was used. Since the rate of initiation with  $\text{A}_3$  is comparable with the rate of propagation, whenever  $\text{A}_3$  is used the number of used  $\text{O}^i\text{Pr}$  groups is equal to 3. This conclusion, based on the  $^1\text{H}$  and  $^{27}\text{Al}$  NMR work, described partially in our preliminary reports and in previous paragraphs, is further evidenced in the present section by means of the molecular weight measurements.

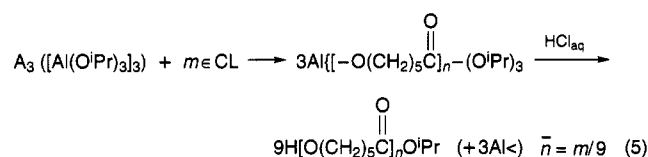
The  $^1\text{H}$  NMR spectrum of poly( $\epsilon\text{CL}$ ) prepared with 95%  $\text{A}_3$  (Figure 2a) shows that practically all of the  $\text{O}^i\text{Pr}$  groups in the starting  $\text{A}_3$  are transformed into the poly( $\epsilon\text{CL}$ ) end groups. This result suggests that in the active all three alkoxide groups propagate and that three chains are attached to every Al atom. Therefore, the molecular weight ( $\bar{M}_n$ ) of the living poly( $\epsilon\text{CL}$ ) should be 3 times larger than  $\bar{M}_n$  of the polymer chains obtained after deactivation of the living system. Thus,  $\bar{M}_n$  of the resulting poly( $\epsilon\text{CL}$ ), after hydrolysis of the growing aluminum trialkoxide, should be equal to

**Table 3. Molecular Weights ( $\bar{M}_n$ ) and Their Distributions ( $\bar{M}_w/\bar{M}_n$ ) for Poly( $\epsilon$ CL) Prepared with A<sub>3</sub> or A<sub>4</sub> (THF Solvent, 25 °C)**

$[\epsilon\text{CL}]_0$ (mol·L <sup>-1</sup> )	initiator	$x[A_x]_0^a$ (10 <sup>-3</sup> mol·L <sup>-1</sup> )	polym time (min)	$\bar{M}_n(\text{calcd})^b$	$\bar{M}_n(\text{GPC})^{c,d}$	$\bar{M}_w/\bar{M}_n(\text{GPC})^d$	$x[A_x]_c^g$ (10 <sup>-3</sup> mol·L <sup>-1</sup> )
1.47	A <sub>3</sub>	0.49	~1000	118 997	108 000	1.03	0.52
2.02		1.01	260	76 093	87 000	1.05	0.88
1.80		1.62	90	42 175	41 000	1.15	1.67
2.02		2.20	60	34 870	40 500	1.10	1.90
2.02		2.99	25	25 682	28 000	1.11	2.74
1.99	A <sub>4</sub>	4.03	15	18 796	22 000	1.09	3.49
2.00		4.00	~4000	19 023	280 000 <sup>e,f</sup>	—	0.27
2.00		29.60	~2000	2 631	49 400 <sup>f</sup>	1.45	1.54
2.00		54.20	1000	1 464	36 400 <sup>f</sup>	1.51	2.09
1.96		110.30	30	736	20 800 <sup>f</sup>	1.91	3.59

<sup>a</sup>  $x[A_x]_0$  denotes starting concentration of a given aggregate ( $x = 3$  or  $4$  for trimer or tetramer, respectively) in terms of the Al(O<sup>i</sup>Pr)<sub>3</sub> unit content. <sup>b</sup>  $\bar{M}_n(\text{calcd}) = ([\epsilon\text{CL}]_0/3 \times x[A_x]_0 \times 114.14 + 60.10)$ , where 114.14 and 60.10 are the molecular weights of  $\epsilon$ CL and 2-propanol, respectively. <sup>c</sup> Absolute values—light scattering and RI detectors in series. <sup>d</sup> Measured for poly( $\epsilon$ CL) deactivated with HCl<sub>aq</sub> ( $\dots\text{CH}_2\text{O})_3\text{Al} \rightarrow 3\dots\text{CH}_2\text{OH}$ ). <sup>e</sup> Measured with a membrane osmometer. <sup>f</sup>  $\bar{M}_n(\text{GPC})$  measured for the polymers isolated at the moment of  $\epsilon$ CL “complete” consumption. However, when the polymerizing mixtures were then kept longer under the living conditions,  $\bar{M}_n(\text{GPC})$  eventually approached  $\bar{M}_n(\text{calcd})$ , calculated by assuming full conversion of A<sub>4</sub> (cf. Figures 4 and 7). <sup>g</sup>  $x[A_x]_c$  denotes concentration of the consumed initiator, calculated on the basis of the measured molecular weight of the resulting polymer, i.e.,  $x[A_x]_c = 114.14[\epsilon\text{CL}]_0/3(\bar{M}_n(\text{GPC}) - 60.10)$ .

$([\epsilon\text{CL}]_0/3 \times 3[\text{Al}_3]_0)\text{MW}_{\epsilon\text{CL}} + \text{MW}_{\text{PrOH}}$  (where  $\text{MW}_{\epsilon\text{CL}} = 114.14$  and  $\text{MW}_{\text{PrOH}} = 60.10$  are the molecular weights of  $\epsilon$ CL and isopropyl alcohol, respectively). This simple relation is illustrated:



<sup>1</sup>H NMR measurements revealed, however, that initiation with A<sub>3</sub> is almost but not fully quantitative (cf. Table 2). It appears that a certain small fraction of A<sub>3</sub> is transformed during initiation into A<sub>4</sub>, within a time insufficient to observe any A<sub>3</sub> → A<sub>4</sub> conversion when monomer is absent, but otherwise the conditions are identical. This would mean that during initiation the rate of A<sub>3</sub> → A<sub>4</sub> transformation is higher than in solution without monomer. This preliminary observation has to be confirmed quantitatively. The reasons for this difference will be discussed elsewhere.<sup>29</sup>

Therefore, in calculations of the predicted molecular weights ( $\bar{M}_n(\text{calcd})$ ) we used, instead of  $[A_3]_0$ , the  $[A_3]_c$ , where  $[A_3]_c$  is the concentration of the consumed A<sub>3</sub> determined from the <sup>1</sup>H NMR spectra of the polymerizing mixtures, after subtracting from  $[A_3]_0$  the concentration of the A<sub>4</sub> left in the system after the polymerization is over (Table 2).

Similarly, in polymerizations initiated with A<sub>4</sub>, the  $\bar{M}_n(\text{calcd})$  were calculated using  $[A_4]_c$  obtained by subtracting from  $[A_4]_0$  the concentration of the unreacted A<sub>4</sub>.

Finally, the values of  $\bar{M}_n(\text{calcd})$  and  $\bar{M}_n$  determined by GPC ( $\bar{M}_n(\text{GPC})$ ) and <sup>1</sup>H NMR ( $\bar{M}_n(\text{NMR})$ ), from the concentration of the  $\dots\text{CH}_2\text{OH}$  and  $\dots\text{C}(\text{O})\text{OCH}(\text{CH}_3)_2$  end groups, for poly( $\epsilon$ CL) deactivated with HCl<sub>aq</sub> are compared in Table 2. The predicted and measured values are in a good agreement.

Table 2 presents data for a relatively high  $[\text{Al}(\text{O}^i\text{Pr})_3]_0 = 7 \times 10^{-2}$  mol·L<sup>-1</sup>, in order to enhance the NMR observations. On the other hand, in Table 3, containing data for  $[\text{Al}(\text{O}^i\text{Pr})_3]_0 \leq 4 \times 10^{-3}$  mol·L<sup>-1</sup>,  $\bar{M}_n(\text{calcd})$  were calculated assuming that all O<sup>i</sup>Pr groups from either A<sub>3</sub> or A<sub>4</sub> are converted into the poly( $\epsilon$ CL) end groups (quantitative initiation). Again, there is relatively good agreement between the calculated and measured values

of  $\bar{M}_n$  for A<sub>3</sub> (here,  $\bar{M}_n(\text{calcd})$  is not corrected as in Table 2) and an obvious disagreement for A<sub>4</sub>.

In polymerizations initiated with A<sub>4</sub>, the determined values of  $\bar{M}_n$  ( $\bar{M}_n(\text{GPC})$ , Table 3) show that the large majority of A<sub>4</sub> (above 90 mol %, as calculated from the resulting  $\bar{M}_n$ ,  $4[A_4]_c = 114.14[\epsilon\text{CL}]_0/3(\bar{M}_n(\text{GPC}) - 60.10)$  (Table 3), remains unreacted once  $\epsilon$ CL is consumed. The molecular weight distributions are considerably broader than with A<sub>3</sub>; this may be related to the slow initiation.

Moreover, in polymerizations initiated with A<sub>4</sub>,  $\bar{M}_n$  is reduced after  $[\epsilon\text{CL}]$  reaches its equilibrium concentration and the reaction mixture is maintained at the monomer  $\rightleftharpoons$  living polymer  $\rightleftharpoons$  cyclic oligomer equilibrium (Figure 7). The equilibrium monomer concentration ( $[\epsilon\text{CL}]_{\text{eq}}$ ) is equal to  $5 \times 10^{-3}$  mol·L<sup>-1</sup> at 25 °C, as calculated from the thermodynamic data given in ref 30. At these conditions, the unreacted A<sub>4</sub> molecules initiate polymerization with monomer and cyclic oligomers present at equilibrium, longer chains depropagate, and new chains are formed at their expense. The direct reaction of A<sub>4</sub> with the linear polymer cannot be excluded (cf. also Figure 4).

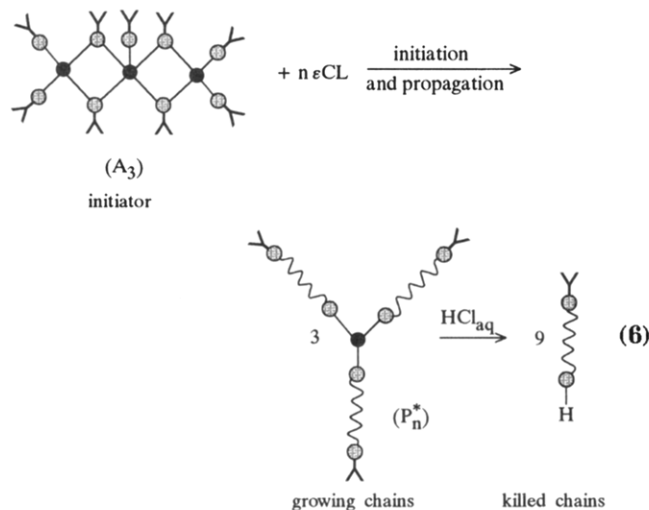
**Structure of the Active Centers.** Results presented in the previous sections have shown that three chains grow from one aluminum atom and that either A<sub>3</sub> or A<sub>4</sub> is capable of providing quantitative initiation. However, the kinetics differ; i.e., A<sub>3</sub> is fast and A<sub>4</sub> is very slow. Nevertheless, the actual mechanism of initiation and the corresponding rate constants of initiation with A<sub>3</sub>, A<sub>4</sub>, or both are not yet known and are being studied. If enough time is given then all of the O<sup>i</sup>Pr groups are incorporated into the living chains, independently, whether A<sub>3</sub>, A<sub>4</sub>, or their mixture is used in initiation.

In this section we present further arguments showing that indeed there are three chains growing from one aluminum atom. These arguments are based on the following measurements: first  $\bar{M}_w$  of the living growing macromolecules were measured by light scattering and then the living species were killed—i.e., individual chains of the aluminum tri(macroalkoxide)s were cutoff from the Al atom and the  $\bar{M}_n$  of these individual chains measured.

The  $\bar{M}_w$  of poly( $\epsilon$ CL) prepared with A<sub>3</sub> and measured by a MALLS light scattering method are given in Table 4; the corresponding Zimm plots for the living polymers are shown in Figure 8. Since indexes of the polydispersity ( $\bar{M}_w/\bar{M}_n$ ) of the killed polymers are close to 1,

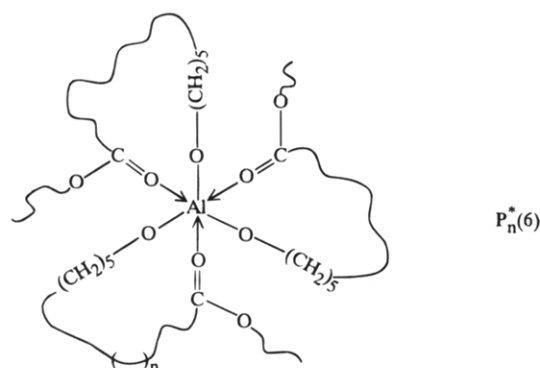


similar values of  $\bar{M}_w/\bar{M}_n$  could be assumed for the living polymers and, therefore, practically  $\bar{M}_w(\text{MALLS}) \approx \bar{M}_n$ . As it follows from Table 4, the predicted and measured values of  $\bar{M}_n$  for the killed polymers are close, and the respective values for the living polymers are approximately 3 times higher. Thus, it follows that the growing macromolecules form three-armed branched structures; i.e., three chains grow on one Al atom, as presented schematically:



(where the black circle and the grey circle denote the Al and O atom, respectively;  $\sim$  denotes the <sup>1</sup>Pr group and  $\sim\sim\sim$  the poly( $\epsilon$ CL) macromolecule).

The <sup>27</sup>Al NMR spectra of the living poly( $\epsilon$ CL) (Figure 6a,b) initiated with A<sub>3</sub> exhibit a strong band at  $\delta \approx 5$  ppm. This is the absorption range characteristic for the hexacoordinated Al atoms. Thus, in the active species, having a structure of the monomeric aluminum trimacroalkoxide, the additional coordination of the trivalent Al atom takes place in such a way that the coordination number increases to six. This coordination may proceed with the acyl oxygen atoms of the poly( $\epsilon$ CL) repeating units, as in the structure P<sub>n</sub><sup>\*</sup>(6):

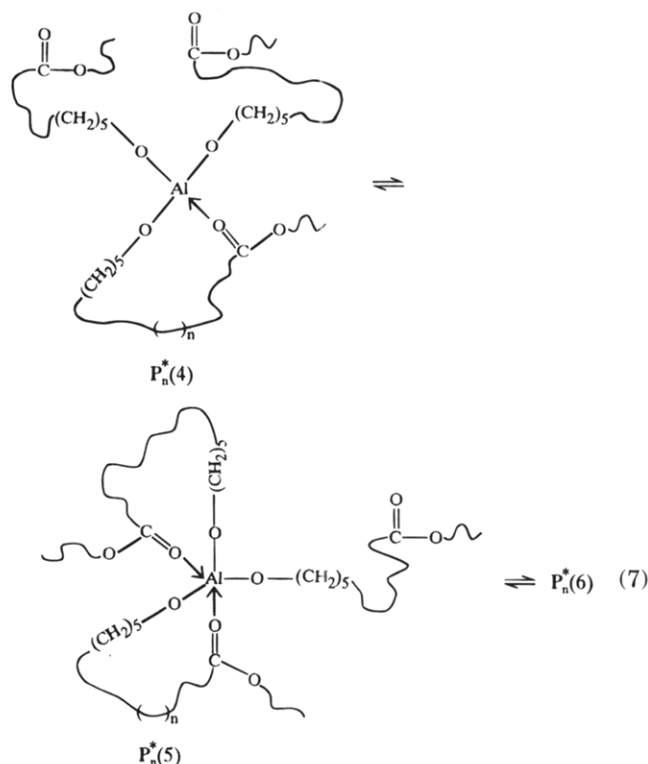


The average number  $\bar{n}$  in the figure is not yet known and is under study. It is, however, highly possible that for the entropic reason this is the last unit providing the carbonyl group for coordination and  $n = 0$ .

Similar structures have recently been proposed, assuming however only one growing poly( $\epsilon$ CL) chain from one Al atom.<sup>31</sup> This one chain should then have given three coordination sites.

In the same <sup>27</sup>Al NMR spectrum of the active species, there is also a broad signal present at  $\delta \approx 60$  ppm, i.e., in the Al(4) absorption range. This may be due to the

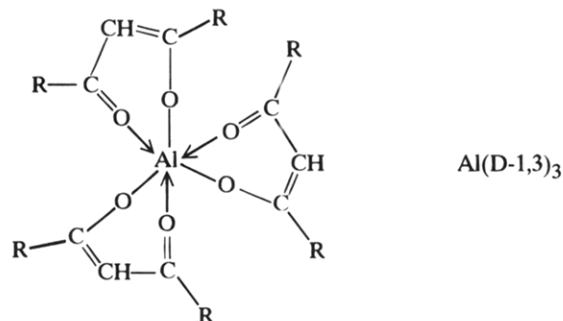
equilibrium (7) in which the tetra- and hexacoordinated species dominate.



Since propagation is first order in the growing species and internally first order in monomer, these two facts indicate, the activity of the average growing species does not depend on the polymerization degree of macromolecules. This, in turn, indicates, that the actual equilibrium between species of various states of solvation is achieved at low DP<sub>n</sub> (i.e. early stage of monomer consumption).

It is known<sup>13,14,26</sup> that Al atoms prefer to be tetra- or hexacoordinated, whereas the pentacoordinated ones are much less abundant and labile.

The P<sub>n</sub><sup>\*</sup>(6) structure given above resembles that of dionates-1,3:<sup>12-14</sup>



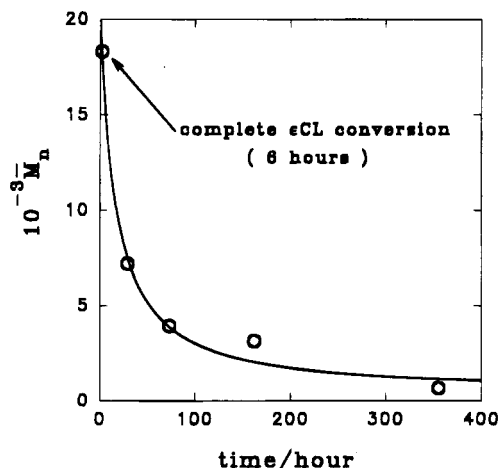
However, the nucleophilicity and complexing ability of the acetyl oxygen atoms in dionates (electron-donating neighboring double bond) is much higher, and therefore, these species are known to be quite stable and not reactive. It may also happen that from the population of corresponding species that species with a coordination number lower than 6 are momentarily active (e.g., P<sub>n</sub><sup>\*</sup>(4) active but P<sub>n</sub><sup>\*</sup>(6) is not). Further work should allow correlation of the rates to the concentrations of the observed corresponding species (P<sub>n</sub><sup>\*</sup>(4), P<sub>n</sub><sup>\*</sup>(5), P<sub>n</sub><sup>\*</sup>(6)).



**Table 4.** Comparison of  $\bar{M}_w$  of Living Poly( $\epsilon$ CL) [ $(\dots-\text{CH}_2\text{O})_3-\text{Al}$ ] with Molecular Weights of Deactivated Poly( $\epsilon$ CL) ( $\dots-\text{CH}_2\text{OH}$ )<sup>a</sup>

[ $\epsilon$ CL] <sub>0</sub> (mol·L <sup>-1</sup> )	3[A <sub>3</sub> ] <sub>0</sub> (10 <sup>4</sup> mol·L <sup>-1</sup> )	10 <sup>-5</sup> $\bar{M}_n$				
		calcd <sup>a</sup> (living)	MALLS <sup>b</sup> (living)	calcd <sup>c</sup> (deactivated)	GPC <sup>d,e</sup> (deactivated)	$\bar{M}_w/\bar{M}_n$ (GPC) (deactivated)
1.47	4.9	3.57	3.16	1.19	1.08	1.03
2.00	12.9	1.77	1.65	0.59	0.65	1.05

<sup>a</sup> Initiator, A<sub>3</sub>; solvent, THF; 25 °C. <sup>b</sup>  $\bar{M}_n$ (calcd), living = ([ $\epsilon$ CL]<sub>0</sub>/3[A<sub>3</sub>]<sub>0</sub>) × 114.14. <sup>c</sup>  $\bar{M}_w$ (MALLS) measured by the multiangle laser light scattering in THF as a solvent at 20 °C. <sup>d</sup>  $\bar{M}_n$ (calcd), deactivated  $1/3\bar{M}_n$ (calcd), living. <sup>e</sup> Absolute values, measured by light scattering and RI detectors in series.

**Figure 7.** Kinetics of decreasing of the molecular weight ( $\bar{M}_n$ ) as measured by GPC for the living poly( $\epsilon$ CL), prepared with A<sub>4</sub>. Polymerization conditions given in the caption for Figure 4.

**Kinetic of  $\epsilon$ CL Polymerization Initiated with A<sub>3</sub> or A<sub>4</sub>.** In the final part of this study we measured the kinetics of polymerization of A<sub>3</sub> and A<sub>4</sub> in order to further substantiate the findings of the previous paragraphs.

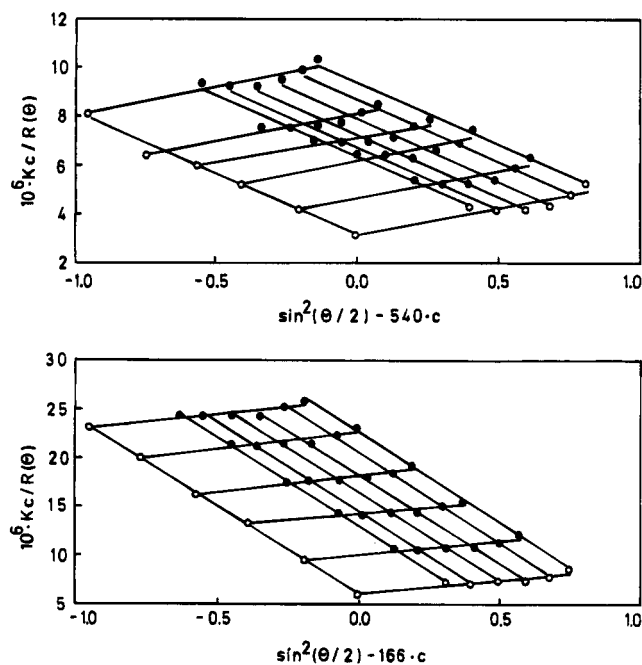
Polymerization of  $\epsilon$ CL initiated with A<sub>3</sub> or A<sub>4</sub> was studied dilatometrically in THF solvent at 25 °C. The starting concentration of  $\epsilon$ CL in all kinetic experiments was  $\sim 2$  mol·L<sup>-1</sup>. Results of the kinetic measurements are presented in Figures 9 and 10 in the form of the semilogarithmic plots:  $\ln([\epsilon\text{CL}]_0/[\epsilon\text{CL}]) = f(\text{time})$ .

In the polymerization initiated with A<sub>3</sub>, the starting concentration of A<sub>3</sub> was changed from  $1 \times 10^{-3}$  to  $4 \times 10^{-3}$  mol·L<sup>-1</sup>. The resulting semilogarithmic plots are either straight lines preceded by a short autoacceleration period or have a sigmoidal shape. In the latter, a short but distinct period to increase in the relative polymerization rate ( $r_p = -d\ln[\epsilon\text{CL}]/dt$ ) is followed by a constant  $r_p$ , and then  $r_p$  decreases. This decrease is particularly apparent for lower starting initiator concentrations, viz. for longer chains. This problem will be discussed elsewhere.

The short acceleration period can be ascribed to the relatively slow initiation. Its origin is being studied and may either be related to the slow initiation by A<sub>3</sub> "as such" or to the slow deaggregation of A<sub>3</sub> to the more reactive species, which is then consumed quickly by monomer.

The propagation rate constant  $k_p = r_p/9[\text{A}_3]_0$  on  $>\text{AlO}(\text{CH}_2)_5\text{C}(\text{O})-\dots$  species is determined from the straight linear plots a–c in Figure 9 and is equal to  $0.62$  mol<sup>-1</sup> L·s<sup>-1</sup> (THF, 25 °C).

In Figure 10, the kinetics with A<sub>4</sub> is illustrated. The semilogarithmic plots,  $\ln([\epsilon\text{CL}]_0/[\epsilon\text{CL}]) = f(\text{time})$ , in polymerizations initiated with A<sub>4</sub> are concave and show

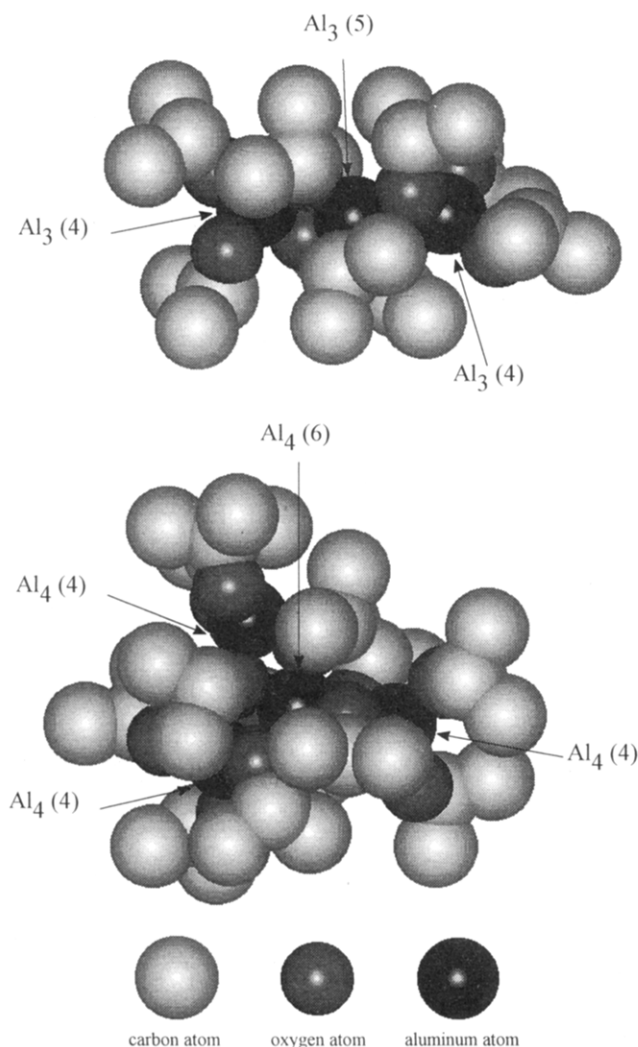
**Figure 8.** Zimm plots obtained for the living poly( $\epsilon$ CL) prepared in  $\epsilon$ CL polymerizations initiated with A<sub>3</sub> (c is the concentration (in g·L<sup>-1</sup>),  $\theta$  the scattering angle,  $K$  an optical constant,  $R(\theta)$  the excess scattered intensity ratio of the solution of concentration  $c$  and at angle  $\theta$ ). Conditions of polymerization: (a) [ $\epsilon$ CL]<sub>0</sub> = 1.47 mol·L<sup>-1</sup>, 3[A<sub>3</sub>]<sub>0</sub> =  $4.9 \times 10^{-4}$  mol·L<sup>-1</sup>, (b) [ $\epsilon$ CL]<sub>0</sub> = 2.0 mol·L<sup>-1</sup>, 3[A<sub>3</sub>]<sub>0</sub> =  $1.29 \times 10^{-3}$  mol·L<sup>-1</sup>; THF as a solvent, and 25 °C.

a gradual increase of  $r_p$  with monomer conversion. This is certainly due to the slow initiation, again, either with A<sub>4</sub> itself or the slowly formed actual initiating species from A<sub>4</sub>. The ratio of the initial  $r_p$ , determined for the polymerizations initiated with A<sub>3</sub> and A<sub>4</sub>, which can be used as a measure of the  $k_{13}/k_{14}$  ratio, gave the value of  $\sim 10^3$  ( $[\text{Al}(\text{O}^i\text{Pr})_3]_0 = 0.1$  mol·L<sup>-1</sup>; THF, 25 °C). This rather rough estimation is based on the graphical determination of the slopes at the earliest stages of polymerization.

Thus, results of these preliminary kinetic studies support the main conclusions derived from the NMR studies, namely, that A<sub>3</sub> is much more reactive than A<sub>4</sub> in their reactions with  $\epsilon$ CL and that the A<sub>3</sub>  $\rightleftharpoons$  A<sub>4</sub> interconversion rates are low in comparison with the  $\epsilon$ CL polymerization rates.

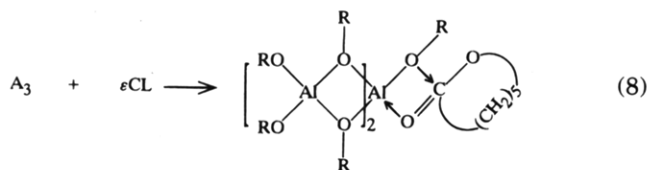
Although the series of elementary reactions from A<sub>3</sub> and A<sub>4</sub> to the final operating growing species are not yet known, the reactivity difference between A<sub>3</sub> and A<sub>4</sub> seems to be related to the different coordination numbers of the central Al atoms in both aggregates. The highly stable structure of A<sub>4</sub>, discussed in this paper, results from the presence of the hexacoordinated Al atoms in the center of A<sub>4</sub>. These are known to be stable because of the complete filling of the coordinate sphere of Al in Al(6). The presence of the pentacoordinated Al

atom in the center of the trimer ( $A_3$ ) makes this aggregate much less stable since there is no structural possibility of forming  $Al(6)$  in  $A_3$ . These structures, calculated according to the force field MM+ method employing the Hyperchem computer program,<sup>32</sup> are compared below ( $A_3$  followed by  $A_4$ ); the resulting  $A_4$  structure is close to that determined by a single crystal X-ray diffraction.<sup>33</sup>



It is clearly seen that the central Al atom in  $A_4$  ( $Al_4(6)$ ) is stable not only by its hexacoordinated nature but also because of the steric inaccessibility.

Both  $A_3$  and  $A_4$  contain the outer, tetracoordinated Al atoms ( $Al(4)$ ). Therefore,  $Al(4)$  is expected not be involved in the rate-determining step of the  $A_3$  breakdown. Probably  $A_3$  tends to expand the uncommon  $Al(5)$  coordination via the bimolecular reaction, (cf. eq 8).



The centrosymmetric  $A_4$  structure could hardly expand coordination of its  $Al(4)$  and  $Al(6)$  atoms by a similar reaction, requiring  $Al(4) \rightarrow Al(5)$  or  $Al(6) \rightarrow Al(7)$  transitions. Nevertheless, Shiner et al.<sup>20</sup> proposed, on the basis of kinetic studies of  $A_3 \rightleftharpoons A_4$  interconversion and reactions of  $A_3$  and  $A_4$  with 2-propanol and

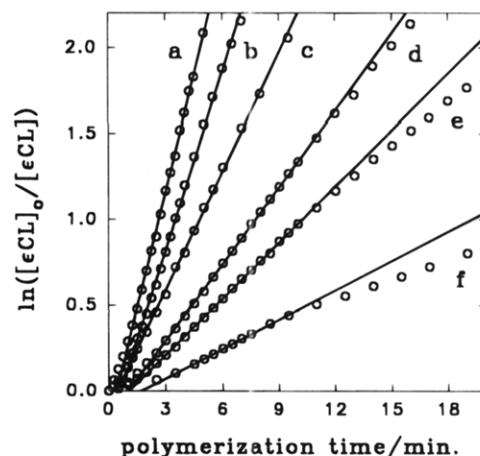


**Figure 9.** Kinetics of  $\epsilon$ CL polymerization initiated with  $A_3$ . Polymerization conditions:  $[\epsilon\text{CL}]_0 \approx 2 \text{ mol}\cdot\text{L}^{-1}$ , THF as solvent,  $25^\circ\text{C}$ , and  $3[A_3]_0$  (in  $10^{-3} \text{ mol}\cdot\text{L}^{-1}$ ) = 4.0 (a), 3.0 (b), 2.2 (c), 1.9 (d), 1.6 (e), and 1.0 (f).

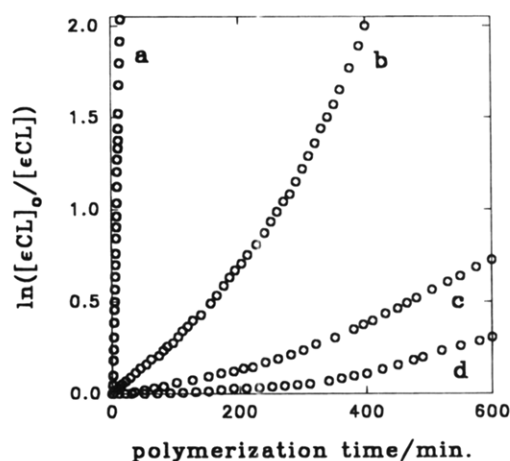
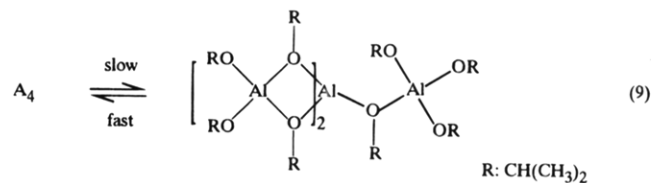


**Figure 10.** Kinetics of  $\epsilon$ CL polymerization initiated with  $A_4$ . Polymerization conditions:  $[\epsilon\text{CL}]_0 = 2 \text{ mol}\cdot\text{L}^{-1}$ , THF as a solvent,  $25^\circ\text{C}$ , and  $4[A_4]_0$  (in  $10^{-3} \text{ mol}\cdot\text{L}^{-1}$ ) = 110 (a), 54 (b), 30 (c), and 4 (d).

ketones, that the rate-determining step in the  $A_4$  disruption is the unimolecular scission of the  $Al(6)$ –oxygen bond (cf. eq 9). The resulting structure, contain-

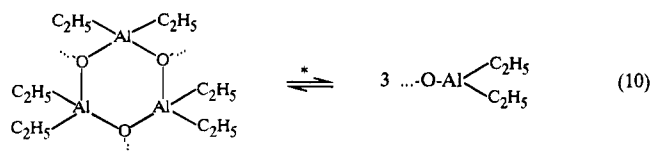


ing  $Al(5)$ , may then undergo a bimolecular reaction with monomer or other nucleophile. This is probably the first step of  $A_4$  rearrangement or breaking down into smaller species.

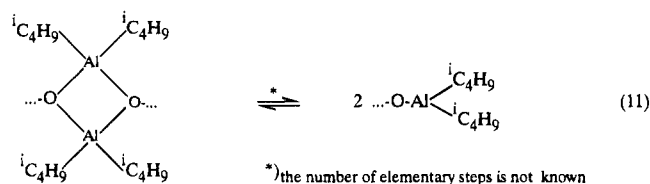
**Comparison of Polymerization of  $\epsilon$ CL Initiated with  $R_2\text{AlOR}'$  and  $\text{Al}(\text{O}^i\text{Pr})_3$ .** Previously, we studied  $\epsilon$ CL polymerization initiated with dialkylaluminum alkoxides ( $R_2\text{AlOR}'$ ).<sup>7,15,35,36</sup> These initiators exist in solutions are aggregates, mostly cyclic dimers or trimers.<sup>12,14</sup> We observed, however, in  $^1\text{H}$  NMR spectra of  $\sim 0.1 \text{ mol}\cdot\text{L}^{-1}$  solutions of  $R_2\text{AlOR}'$  (e.g., of  $(\text{C}_2\text{H}_5)_2\text{AlOCH}_3$ ,  $[(\text{CH}_3)_2\text{CHCH}_2]_2\text{AlOCH}_3$ , and  $(\text{C}_2\text{H}_5)_2\text{AlOCH}_2\text{CH}=\text{CH}_2$ )<sup>7</sup> sharp signals and only one chemical shift for a given group of protons. Such behavior indicates that these initiators either exist exclusively in one aggregated form or interchange fast, on the NMR time

scale, with another aggregate or with the monomeric, nonaggregated species.

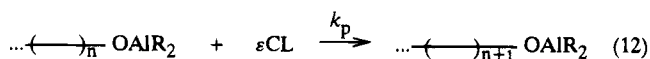
In propagation the active centers, derived from  $R_2AlOR'$ , are aggregated or deaggregated depending on the polymerization conditions. For the aggregated species, their degree of aggregation is dependent on the size of the alkyl substituent, e.g., ethyl aggregates are trimeric



whereas for isobutyl substituents aggregates are dimeric



According to kinetic studies the actual propagation proceeds on the deaggregated species; the order measured in the growing species was  $1/2$  for  $R$  = isobutyl and  $1/3$  for  $R$  = ethyl.



The interconversion between aggregated and nonaggregated species is fast in comparison with propagation, as evidenced from the  $\bar{M}_w/\bar{M}_n$ , usually being below 1.1.<sup>6,7,9</sup> However, the discrete mechanism of deaggregation (a number of steps) is not yet known.

These aggregation  $\rightleftharpoons$  deaggregation phenomena are observed exclusively at higher concentrations of active species. Below a certain concentration the equilibrium is shifted to the deaggregated species; e.g., below  $10^{-3}$  mol·L<sup>-1</sup> there is above 90 mol % of these species for equilibrium 10 or 11 (THF, 25 °C).<sup>36</sup> For this reason, polymerization from the fractional order with respect to the growing species (viz. initiator) becomes first order. The rate constants of propagation ( $k_p$ ) determined for these two distinctive regions of concentrations are in good agreement (e.g., for  $\text{Et}_2\text{AlOEt}$  in THF as a solvent at 25 °C the values of  $0.039 \pm 0.001$  and  $0.048 \pm 0.005$  mol<sup>-1</sup>L·s<sup>-1</sup> have been obtained, respectively) although the method of calculation differs;<sup>36</sup> this is a strong argument for correctness of the kinetic treatment.

Aggregates can also be disrupted by addition of strongly complexing agents or by using solvents (e.g., acetonitrile<sup>15</sup>) interacting strongly enough with aggregates to displace homoligands. This is possible, because all of the aggregates formed from  $R_2AlO\cdots$  are weakly kept together by merely two oxygen atom bridges per one aluminum atom and, therefore, easily give back the deaggregated more or less strongly solvated species.

The aluminum trialkoxides form much stronger aggregates. The number of components in the starting initiators (dimers, trimers, tetramers, etc.) depends on the size of substituents, solvent, and concentration.<sup>12-14</sup>  $\text{Al}(\text{O}^i\text{Pr})_3$  is known to exist mostly as a mixture of trimers ( $A_3$ ) and tetramers ( $A_4$ ) at various compositions in the large majority of systems.

These aggregates are much stronger and therefore much less labile than the aggregates of  $R_2AlOR'$ . This is because there are in more than two oxygen atom bridges available, linked to one aluminum atom. This number goes up to six in the central Al atom in  $A_4$ . Thus, not surprisingly, the  $A_3 \rightarrow A_4$  interconversion is slow in comparison with  $\epsilon\text{CL}$  propagation.

The next problem is the number of macromolecules growing from one Al atom in the involved active centers ( $x$ ). This number has to be distinguished from the average number  $\bar{x}$ , calculated for all of the Al atoms used in initiator. We showed in our earlier paper<sup>7</sup> that in  $R_2AlOR'$ -initiated  $\epsilon\text{CL}$  polymerization only  $R'O$  groups are involved in initiation and transferred to the polymer chain quantitatively as the head end groups; i.e., from one Al atom there is one poly( $\epsilon\text{CL}$ ) macromolecule ( $x = 1$ ) growing, as is visualized in eqs 10-12.

In the present work we have shown that in the  $A_3$ -initiated polymerizations of  $\epsilon\text{CL}$  the initiator reacts entirely; i.e., all of its  $\text{O}^i\text{Pr}$  groups are transformed into the poly( $\epsilon\text{CL}$ ) head end groups ( $x = 3$ ).  $A_3$  has been shown to be much more reactive than  $A_4$ . Therefore, when a mixture of  $A_3$  and  $A_4$  is used, the  $A_3$  is consumed completely, whereas  $A_4$  is left unreacted. Based on the amount of initiator used, the calculated average  $\bar{x}$  value may be well below 3. The same is observed in the polymerizations initiated with  $A_4$  alone, where  $\bar{x}$  may attain any number above 0 and below 3, depending on the conditions of polymerization. It has to be stressed, however, that finally  $A_4$  also generates active species in which all three alkoxide groups linked to one Al atom do propagate ( $x = 3$ ). The difference between  $A_3$  and  $A_4$  is exclusively related to the rates of initiation, and finally, the resulting active centers have the identical structure; thus,  $x = 3$ , although  $0 < \bar{x} \leq 3$ .

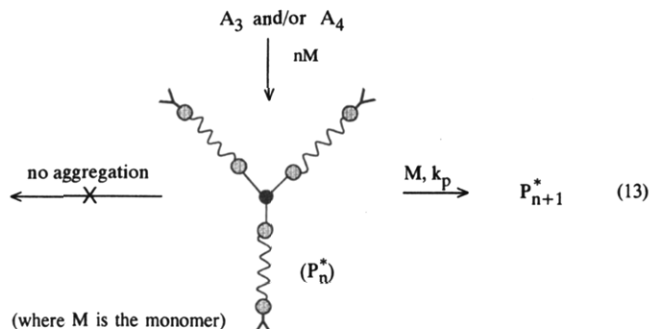
Kricheldorf et al.<sup>8</sup> found, in the bulk polymerization of  $\epsilon\text{CL}$  at 100 °C initiated with  $\text{Al}(\text{O}^i\text{Pr})_3$ , three poly( $\epsilon\text{CL}$ ) chains propagating on one Al atom. The <sup>1</sup>H NMR (100 MHz) spectra of the initiator were reported to show only one doublet and septet in the 6:1 ratio due to the  $-\text{CH}_3$  and  $>\text{CH}$  protons, respectively. Thus, in agreement with our <sup>1</sup>H NMR data,<sup>16</sup> it was mostly a trimer of  $\text{Al}(\text{O}^i\text{Pr})_3$  that was fully consumed in polymerization.

Another group reported<sup>3,18,37</sup>  $\bar{x}$  from 0.9 to 1.4 for the temperature range from 0 to 100 °C, working apparently with the  $A_3/A_4$  mixture.

Monomers less reactive than  $\epsilon\text{CL}$ , such as lactides,<sup>38</sup> requiring higher polymerization temperatures may give  $A_4$  enough time to be consumed before monomer polymerizes completely, and therefore  $\bar{x} \approx 3$  for any  $A_3$  and  $A_4$  concentration ratio. However, as we have observed recently,<sup>29</sup> these two aggregates react also with lactides with different rates ( $k_{13}/k_{14} \approx 50$ ).

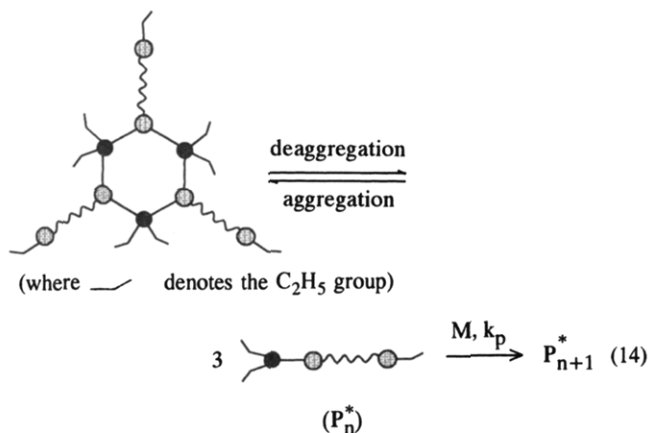
In the presence of 2-propanol, three alkoxide groups per one Al atom were found to propagate ( $\bar{x} = 3$ ).<sup>3,18</sup> This can be explained by our recent observation<sup>22</sup> that, in  $\epsilon\text{CL}$  polymerization conducted in the presence of alcohols and diols,  $A_4$  is completely consumed, because alcohols break down  $A_4$  relatively fast to the more reactive species.

Thus, when initiation takes place and aluminum isopropoxide aggregates ( $A_3$  and/or  $A_4$ ) react with monomer, then finally, at a stage not yet known, the Al atom carries three chains. The presence of three chains eliminates aggregation (schematically):



The structure of  $P_n^*$  in (13) is an oversimplification. As has been discussed, the growing species are probably self-solvated by the first polymer repeating unit linked to the Al atom. This self-solvation provides, according to the  $^{27}\text{Al}$  NMR spectra, the tetra- and hexacoordinated species (cf.  $P_n^*(4)$  and  $P_n^*(6)$  in eq 4). Then,  $P_n^*(6)$  may not be reactive and  $P_n^*(4)$  may propagate (the presence of  $P_n^*(5)$  is not excluded, however, but not yet determined). The internal first order in monomer indicates that the  $[P_n^*(4)]/[P_n^*(6)]$  ratio becomes invariant at the very early stages of polymerization. If this is true, the rate constants measured will only be apparent ones.

In polymerization on  $\text{R}_2\text{AlOR}'$ , there is only one chain growing from an Al atom. Therefore, there is still the ability to aggregate left, since there is enough room to accommodate one or two (for  $\text{R} = \text{C}_4\text{H}_9$  or  $\text{R} = \text{C}_2\text{H}_5$ , respectively) more homocomponents, e.g.:



The self-solvation of these species, in analogy with  $P_n^*(4)$ ,  $P_n^*(5)$ , and/or  $P_n^*(6)$  is a matter of further studies.

**Acknowledgment.** The authors thank Dr. M. Potrzebowski from the Center of Molecular and Macromolecular Studies for the valuable discussions and help related to the NMR measurements.

## References and Notes

- (1) Cox, F. E.; Hostettler, F. (Union Carbide Corp.) U.S. Patent 3 021 313, 1962.

- (2) Cherdron, H.; Ohse, H.; Korte, F. *Makromol. Chem.* **1962**, 56, 187.
- (3) Ouhadi, T.; Stevens, Ch.; Teyssié, Ph. *Makromol. Chem. Suppl.* **1975**, 1, 191.
- (4) Vion, J.-M.; Jérôme, R.; Teyssié, Ph.; Aubin, M.; Prud'homme, R. E. *Macromolecules* **1986**, 19, 1828.
- (5) Hsieh, H. L.; Wang, I. W. *ACS Symp. Ser.* **1984**, No. 286, 161.
- (6) Hofman, A.; Słomkowski, S.; Penczek, S. *Makromol., Rapid Commun.* **1987**, 8, 387.
- (7) Duda, A.; Florjańczyk, Z.; Hofman, A.; Słomkowski, S.; Penczek, S. *Macromolecules* **1990**, 23, 1640.
- (8) Kricheldorf, H. R.; Berl, M.; Scharnagl, N. *Macromolecules* **1988**, 21, 286.
- (9) Dubois, Ph.; Jérôme, R.; Teyssié, Ph. *Polym. Bull. (Berlin)* **1989**, 22, 475.
- (10) Wurm, B.; Keul, H.; Hoecker, H. *Macromol. Chem. Phys.* **1994**, 195, 3489.
- (11) Löfgren, A.; Albertsson, A.-C.; Dubois, Ph.; Jérôme, R.; Teyssié, Ph. *Macromolecules* **1994**, 27, 5556.
- (12) Mole, T.; Jeffery, E. A. *Organosilicon Compounds*; Elsevier: Amsterdam, 1972; p 214.
- (13) Bradley, D. C.; Mehrotra, R. C. Gaur, D. P. *Metal Alkoxides*; Academic Press: London, 1978; pp 74, 122.
- (14) Eisch, J. J. *Aluminum*. In *Comprehensive Organometallic Chemistry*; Wilkinson, G., Stone, F. G. A., Abel, E. W., Eds.; Pergamon Press: Oxford, U.K., 1982; Vol. 1, p 583.
- (15) Penczek, S.; Duda, A.; Biela, T. *Polym. Prepr. (Am. Chem. Soc., Div. Polym. Chem.)* **1994**, 35(2), 508.
- (16) Duda, A.; Penczek, S. *Macromol. Rapid Commun.* **1995**, 16, 67.
- (17) Szymanski, R.; Duda, A.; Penczek, S., in preparation.
- (18) Jacobs, C.; Dubois, Ph.; Jérôme, R.; Teyssié, Ph. *Macromolecules* **1991**, 24, 3027.
- (19) Baran, T.; Duda, A.; Penczek, S. *Makromol. Chem.* **1984**, 185, 2337.
- (20) Kleinschmidt, D. C.; Shiner V. J.; Whittaker, D. J. *Org. Chem.* **1973**, 38, 3334.
- (21) Ropson, N.; Dubois, Ph.; Jérôme, R.; Teyssié, Ph. *Macromolecules* **1993**, 26, 6378.
- (22) Duda, A., to be published.
- (23) Duda, A.; Penczek, S. *Polym. Prepr. (Am. Chem. Soc., Div. Polym. Chem.)* **1990**, 30(1), 12.
- (24) DeSimone, J. M.; Stangle, M.; Riffle, J. S.; McGrath, J. E. *Macromol. Chem., Macromol. Symp.* **1991**, 42/43, 373.
- (25) Arai, T.; Inoue, S. *Tetrahedron* **1990**, 46, 749.
- (26) Benn, R.; Rufinska, A. *Angew. Chem., Int. Ed. Engl.* **1986**, 25, 861.
- (27) Akitt, J. W.; Duncan, R. H. *J. Magn. Reson.* **1974**, 15, 162.
- (28) Křiž, O.; Čáslenský, B.; Lyčka, A.; Fusek, J.; Heřmánek, S. *J. Magn. Reson.* **1984**, 60, 375.
- (29) Tokar, R.; Duda, A.; Penczek, S., in preparation.
- (30) Lebedev, B. V.; Yevstropov, A. A.; Lebedev, N. K.; Karpova, E. A.; Lyudvig, E. B.; Belenkaya, B. G. *Vysokomol. Soed., Ser. A* **1978**, 20, 1974.
- (31) Ropson, N. Ph.D. Thesis, University of Liège, Liège, Belgium, 1994.
- (32) Hyper Chem™ Release 2 for Windows. *Reference Manual*; Autodesk, Inc. 1992; p 169.
- (33) Turova, N. Ya.; Kozunov, V. A.; Yanowskii, A. I.; Bokii, N. G.; Struchkov, Yu. T.; Tarnopol'skii, B. L. *J. Inorg. Nucl. Chem.* **1979**, 41, 5.
- (34) Shiner, V. J.; Whittaker, D. J. *Am. Chem. Soc.* **1969**, 91, 394.
- (35) Duda, A.; Penczek, S. *Makromol. Chem., Macromol. Symp.* **1991**, 47, 127.
- (36) Duda, A.; Penczek, S. *Macromol. Rapid Commun.* **1994**, 15, 559.
- (37) Ropson, N.; Dubois, Ph.; Jérôme, R.; Teyssié, Ph. *Macromolecules* **1994**, 27, 5950.
- (38) Dubois, Ph.; Jacobs, C.; Jérôme, R.; Teyssié, Ph. *Macromolecules* **1991**, 24, 2266.

MA950166Y